Theor Appl Climatol (2016) 124:425–449
DOI 10.1007/s00704-014-1366-x

ORIGINAL PAPER

Search for an astronomical site in Kenya (SASKYA) using climate reanalyses and high-resolution meteorological model data

Edward Graham · Richard Vaughan · David A. H. Buckley · Koi Tirima

Received: 9 June 2014 / Accepted: 28 December 2014 / Published online: 19 March 2015
© Springer-Verlag Wien 2015

Abstract The goal of the Search for an Astronomical Site in Kenya (SASKYA) project is to identify the best possible site(s) in Kenya for astronomical optical observation, using ERA-interim climate reanalyses and high-resolution UK Met Office Africa Limited Area meteorological model (Africa-LAM) data. This initial search focusses on a selection of 13 candidate mountain peaks across Kenya. A mixture of 30 years (1981–2010) of relatively coarse-grained ERA-interim reanalyses data and 12 months' (2011–2012) of much higher resolution UK Met Office Africa-LAM data were used to determine the best possible sites. Cloud cover, precipitable water vapour (specific humidity), vertical velocity, aerosol loadings and wind data were analysed. The results confirm that many sites in Kenya are reasonably cloud free, with estimated photometric night fractions of possibly 50 % at the best sites. Significant seasonal inter-annual and inter-decadal variations in cloud cover can be expected, however. Average precipitable water vapour (PWV) values are uncomfortably high, but periods of much lower PWV can be expected during favourable conditions in the dry seasons. Long-term vertical velocities (as a proxy to determine areas of improved "seeing" conditions) indicate that good astronomical viewing conditions are likely to be dependent on the season and wind direction across Kenya. Finally, after full consideration of the climatological data, a trade-off is expected between the best possible site in climatological terms, and the practicalities of installing remote equipment in isolated, inaccessible areas with little or no infrastructure.

E. Graham (✉)
Lews Castle College, University of the Highlands and Islands,
Stornoway HS2 0XR, Na h-Eileanan an Iar, Scotland
e-mail: edward.graham@uhi.ac.uk

D. A. H. Buckley
South African Astronomical Observatory, Observatory,
Cape Town 7925, South Africa

R. Vaughan
InCA Nairobi Ltd, Centenary House, 3rd Floor, Westlands,
P.O. Box 97, 00606 Nairobi, Kenya

K. Tirima
Inoorero Centre, Inoorero University, Parklands,
P.O. Box 60550-00200, Nairobi, Kenya

1 Introduction

The goal of the Search for an Astronomical Site in Kenya (SASKYA) project is to identify the best possible site(s) in Kenya for optical astronomical observation, using state-of-the-art climate reanalyses and other high resolution meteorological model data. At present, there are few major telescopes available for research use in the whole of central and eastern Africa, and the aim of SASKYA is to determine whether a suitable site can be found in Kenya for a research telescope of 1–2 m in diameter, using meteorological model and climatological datasets.

This initial search is focussed on a selection of candidate mountain peaks in the centre and in the north of the country. If realised, the building of such a telescope would provide a much-needed scientific, technological and economic boost to Kenya, particularly for students with an interest in physics or astronomy who currently have to move elsewhere for any kind of practical experience.

Kenya already hosts a node of the Square Kilometer Array (SKA) and participates in the African Very Long Baseline Interferometry (VLBI) Network (AVN) using existing decommissioned radio telecommunications dishes. SASKYA therefore increases the opportunity for research in Kenya and train more students in astronomy and physics. Above all, the construction of a large telescope in Kenya would enable many

more students from across Africa to remain on their home continent during the duration of their education and training.

1.1 Climatological considerations

Unfortunately, from a climatological perspective, Kenya does not lie within a preferred zone on the Earth's surface for the siting of large telescopes. The most preferable places today all lie within a descending arm of a quasi-permanent sub-tropical high pressure cell [e.g. such as La Silla and Paranal (Atacama, Northern Chile), Izaña and La Palma (Canary Islands), Sutherland (South Africa) and San Pedro Mártir (Baja California); see Figure 6.7.1 of Graham (2008a) for a global identification of these preferable zones]. Instead, Kenya is affected by two annual tropical monsoon seasons per year, which are interspersed by lengthy dry seasons. The monsoon periods in East Africa are, however, highly variable both spatially and temporally, with strong inter-annual and inter-decadal scale variation in intensity (Nicholson 1996). Furthermore, surface humidity and precipitable water vapour values are expected to be uncomfortably high across the country, at least at low to moderate altitudes and during the two annual monsoon seasons.

At the same time, however, the northern and north-eastern portions of Kenya are considerably drier than the south and southwest of the country, with semi-arid to arid conditions predominating across the Chalbi desert (Fig. 1), particularly near the international border with Somalia. Here, there have been severe droughts in recent years (Maxwell and Fitzpatrick 2012), leading to much socio-political upheaval. Janowiak (1988), Anyah and Semazzi (2007) and Marchant et al. (2007) show that Eastern Africa (including most of Kenya) exhibits marked inter-annual and inter-decadal variability in rainfall, which is strongly linked to an Indian Ocean "dipole" (Marchant et al. 2007), and is also related to the prevailing phase of the wider combined atmospheric-oceanic El Nino Southern Oscillation (ENSO) in the tropical Pacific Ocean (Trenberth 1984; Janowiak 1988; Anyah and Semazzi 2007).

1.2 Topography

Kenya is a mountainous country, and much of the western two thirds of the country lie at an altitude of >1,500 m above sea level (ASL), on a plateau known as the Kenyan Highlands (Fig. 1). Within the Highlands, there are numerous larger mountain ranges and peaks, typically rising to between 2000 and 3000 m ASL, although the solitary peak of Mount Kenya (located almost on the equator) rises to a formidable height of 5199 m ASL in a series of rocky peaks. Here, a small but permanent ice cap has persisted for thousands of years (Hastenrath and Kruss 1992; Hastenrath 1995), but it has lost 92 % of its mass during the last century (Mastny 2000; Kaser et al. 2004). There is debate as to whether this is solely due to global warming by greenhouse gases (Hastenrath and Kruss 1992) or partly due

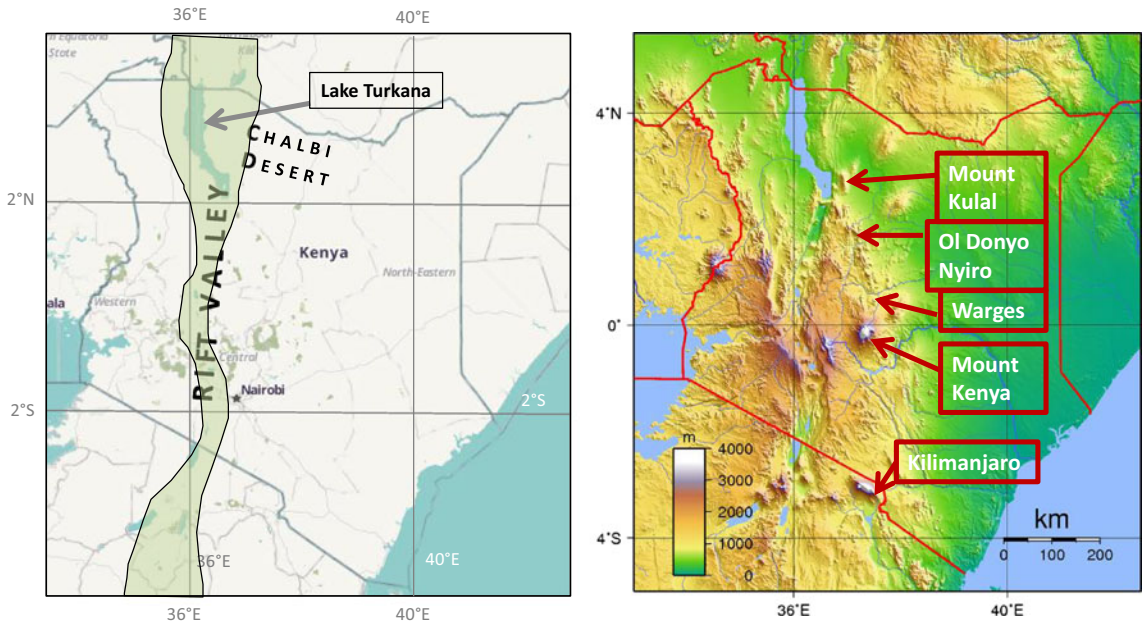

Fig. 1 *Left* Map (source openstreetmap.org) depicting Kenya and the approximate location of the East African Rift Valley, Lake Turkana and the Chalbi desert. *Right* (source Sadalmelik) Kenyan and East African topography and altitude above sea level (metres); the location of five principal mountain summits are also indicated

to regional precipitation change as well (Kaser et al. 2004).

The single most dominant topographic feature in Kenya is the East African Rift Valley, a relatively recent geological feature that cuts a deep swathe through the country from north to south (Fig. 1). Generally speaking, maximum mountain peaks heights are a little higher (~3300 m ASL) west of the Rift Valley than to the east of the valley (~2700 m ASL). As well as posing as a significant topographic feature on the Kenyan landscape, the Rift Valley also marks the approximate boundary between relatively moist and more humid climatic conditions to the southwest [which are sometimes associated with the formation of diurnal thunderstorms near Lake Victoria on the far (western) side of the mountains on the west side of the Rift Valley; Lumb 1970; Yin et al. 2000], and drier and more stable climatic conditions to the north and east of the valley. Lake Turkana, the largest surface water body in Kenya of 6400 km^2, is located at the northern end of Kenyan part of the Rift Valley (Fig. 1).

1.3 Overview of climatological parameters which affect astronomical viewing and their application to SASKYA

Before we present a more detailed analysis of the climatic conditions of Kenya with a view to determining a list of candidate astronomical sites in the country, it is pertinent at this stage to re-consider the main atmospheric constraints and limitations on astronomical viewing (prepared from a comprehensive list, originally detailed by Sarazin 1997). Then, we discuss their application and expected impact on the SASKYA project. The six most important constraints, as summarised by Graham (2008a), consist of the following:

i. Cloud cover
ii. Absorption due to atmospheric water vapour
iii. Stability and turbulence of the atmosphere above the observatory site
iv. Observatory-level night-time relative humidity
v. Appropriate wind speeds at observatory level
vi. Dust and aerosol loadings.

Each of these variables is now considered in turn in relation to the SASKYA project:

i. Cloud cover

It is obvious in saying that night-time cloud-free skies are essential for the successful operation of any optical or infrared astronomical observatory. It is important to add, however, that during the typically longer exposure times of fainter objects, even partially clouded skies are detrimental to observation, as occasional patches of clouds may still drift into the field of view (Graham 2008a), although thinner clouds, such as high level cirrus, can sometimes be tolerated when undertaking differential photometry. Although an obvious initial qualitative association can be made between the percentage of the sky covered in cloud (as determined by satellites and climate reanalyses datasets) and the annual number of photometric nights[1] at any observatory, the relationship is neither clear cut nor is there strong correlation between the two variables over all cloudy ranges, as shown by Graham (2008b) and Graham et al. (2011). However, based on the data presented in Graham (2008b) for the Chilean sites of La Silla and Paranal, there appears to be an approximate negative linear relationship between the ERA-40 reanalysis cloud data and photometric night quality statistics, of the following form:

$$y \cong -1.0x + 80 \quad (1)$$

where x is the mean annual reanalyses cloud cover percentage, and y is the predicted photometric night fraction.

This equation can be tested for observatories outside of Chile. For example, the mean annual ERA-40 reanalyses cloud cover value for a model gridpoint over Baja California (i.e. the reanalysis gridpoint closest to San Pedro Mártir observatory, Mexico) is ≅16 %, based on 13 years of ERA-40 data from 1989 to 2002 (Graham 2008b). Substituting this value into Eq. 1, the predicted photometric night fraction is thus ~64 % for San Pedro Mártir. Interestingly, Tapia (1992) quotes a mean annual photometric night fraction of 56.7 % for San Pedro Mártir observatory, but this is based on observations from an earlier time of 1984–1991. Similarly, Ehgamberdiev et al. (2000) present a mean annual clear night fraction[2] of 58 % for the site of Maidanak (Uzbekistan) based on observations from 1979 to 1985. Based on this figure, Eq. 1 predicts that the ERA-40 reanalyses total cloud cover value should be ~22 %, but Graham (2008b) quotes an equivalent ERA-40 reanalysis value (1989–2002) as much as 36 % for the nearest gridpoint to Maidanak.

Thus, whilst further research is clearly needed on the exact relationship between reanalyses cloud cover and astronomical photometric night fraction statistics, it seems that any relationship between the two variables (based on the above comparisons) can only be regarded as tentative at present; this is also notwithstanding that both datasets are compiled from highly contrasting temporal and spatial information of variable resolution and accuracy. Furthermore, Graham (2008b) notes several important aspects, which adversely affect the accuracy and reliability of the ERA-40 cloud dataset, but these are

[1] A photometric night is generally defined as at least 6 night time hours in a row with sky clear down to 5 degree above horizon (ESO 2007).

[2] Please note here that Ehgamberdiev et al (2000) refer to "clear time" at Maidanak and reserve the phrase "photometric time" for the ESO observatories. Please see Ehgamberdiev et al (2000) for further information.

considerably improved upon in the later ERA-interim dataset (Dee et al. 2011)—the latter which we use in this study.

Bearing all the above considerations in mind, it was therefore decided during SASKYA to search for potential mountain sites with an average ERA-interim sky cloudiness of 30 % or less. According to Eq. 1 (above), this would be equivalent to an estimated photometric night fraction of approximately 50 %. For reference, typical long-term average values of photometric night fractions for the European Southern Observatory Chilean sites include values of 63 % for La Silla and 74 % for Paranal, based on 30 years of data from 1983 to 2013 (ESO 2015). Interestingly, the value for Paranal is given as 77 % for the earlier period 1983–2000 (Casals and Beniston 2001).

ii. Precipitable water vapour

The primary absorber of infrared radiation in the Earth's atmosphere is water vapour, and therefore, knowledge of the total precipitable (integrated) water vapour is very important for astronomical observation. The amount of extinction and distortion at the surface is directly proportional to the water vapour content of the atmosphere (Graham 2008a), particularly in the near infrared.

Sarazin (2003, personal communication) quotes an PWV value of lower than 5 mm as being pre-requisite for the satisfactory operation of large telescopes at visible wavelengths; he also quotes a value of approximately <3 mm being necessary for infrared astronomy, and <1 mm for satisfactory microwave observation. Globally, such low values are only found at the very cold sites of high latitudes (e.g. Antarctica; Lawrence et al. 2004; Agabi et al. 2006) or at high altitude in the dry subtropical deserts (Graham 2008a). Even average PWV values of 5 mm or less will be very difficult to achieve for lengthy periods in Kenya, except on the very high altitude slopes of Mount Kenya.

At the same time, it was decided that searching principally for a site in Kenya with extremely low values of PWV would not become a prerequisite—satisfactory astronomical observation can be still achieved at various wavelengths, such as regularly happens at the South African Astronomical Observatory (SAAO) in Sutherland, South Africa, where the long-term PWV is as high as 7.2 mm (Dr. M. Gaylard, unpublished data, personal communication, 2014).

iii. Stability and turbulence of the atmosphere

The viewing parameter known as "seeing" is widely used by astronomical community to quantify the degree of the "blurriness" of a stellar image over time. Rapid (~milliseconds) variations of the index of refraction of air occur on a range of spatial scales (millimetre to metre) due to atmospheric turbulence. The integrated effect over the path length of light passing through the atmosphere is to produce phase changes of the wavefronts over the entrance pupil of the telescope, resulting in degradation of the Point Spread Function. The exact value of the seeing at any one place and time is largely determined by the stability of the atmosphere and amount of micro-scale thermal turbulence (Sarazin 1997). It is currently not possible to accurately forecast short-term temporal variations of the seeing parameter at an astronomical site, based solely on climatological data, although attempts have been made using high resolution meteorological models with varying degrees of success (e.g. Masciadri and Egner 2004; Environment Canada 2014). On the other hand, however, broad-scale correlation between average seeing and synoptic-scale meteorological air-mass types is possible (Graham 2008a). A detailed profile of the thermal structure of the atmosphere may be obtained by launching radio-sondes (weather balloons) equipped with micro-meteorological instrumentation. The integral of turbulent structures within this profile is directly related to the magnitude of seeing parameter (Ziad 2012).

Hence, during SASKYA, our interest is in determining the location and variability of any zones of gently subsiding (and thus adiabatically warmed) air masses, leading to possible areas of temperature inversion and increased atmospheric stability. The determination of such areas (on a global and international scale) has already been illustrated by Graham (2008a)—here, we will attempt to use the vertical velocity variables of climate reanalyses datasets again to infer spatio-temporal regions of possibly improved seeing conditions across Kenya.

iv. and v. Night-time relative humidity and wind speeds

Night-time relative humidity, if too high, can be detrimental to observation due to the increased risk of deposition of dew or frost on telescopic optics. Similarly, too low or too high wind speeds can preclude observation due to incomplete flushing of the telescope enclosure leading to what is known as thermal or "dome" seeing (light winds), or telescope and enclosure shake (strong winds), respectively. Sarazin (2003, personal communication) quotes that wind speeds should be ideally in the range of 2–8 m/s to prevent either of these two adverse impacts, although some modern observatories can operate up to wind speeds of 14 m/s when observing downwind.

vi. Aerosol and dust loadings

Finally, high aerosol or dust loadings are also problematic for the successful operation of telescopic optics in, or near, desert regions. This is because blowing dust or sand can rapidly degrade telescope mirrors (Giordano and Sarazin 1994) and can also contaminate optical instruments and equipment. Furthermore, atmospheric

extinction is strongly related to dust loadings in the atmosphere (Siher et al. 2004), with shorter wavelengths being most affected due predominantly to Mie scattering, which is inversely proportional to the wavelength. Dust and sandstorms are highly geographically variable across the globe, but it is the Canary Islands' observatories that are most greatly affected by large fluxes of suspended aerosols from the Sahara desert, often several times per year. Other locations, such as the northern Atacama desert (Chile) rarely suffer from such events (Graham 2008a). Fortunately, a long time series (1980–2002) of globally suspended aerosols for low- and mid-latitudes has been enabled by an algorithm first published by Herman et al. (1997) and later developed by Torres et al. (2002), using satellite data from the Total Ozone Mapping Spectrometer (TOMS). The TOMS dataset is available to astronomers in global map or numerical format on the FriOWL software (Graham et al. 2005; Graham 2008a). This extended dataset will be consulted for the purposes of SASKYA.

1.4 Data provenance

We will now consider in detail the various climatological and meteorological model datasets used in SASKYA, in an effort to determine the most suitable candidate sites for a possible optical telescope in Kenya.

The ERA-interim reanalysis dataset used in this study comes from the European Centre for Medium Range Weather Forecasting (ECMWF; Dee et al. 2011). ERA-interim is a more accurate and higher resolution reanalysis product than its predecessor, ERA-40 (Uppala et al. 2005), but it covers a shorter time extent from 1979 to present (ERA-40 has a duration of 45 years from 1957 to 2002).

Reanalyses can be regarded as the most accurate representations of the Earth's atmosphere that are currently available for the past 50 years. They are based on a state-of-the-art numerical weather prediction model combined with a data assimilation scheme, using a wide range of observations from satellites, ships, buoys, weather stations, aeroplanes and weather balloons. The meteorological and climatological variables described by these reanalyses systems have been shown to be valid and satisfactory in most circumstances (Dee et al. 2011; Kalnay et al. 1996; Uppala et al. 2005), although there are shortcomings in some derived variables such as cloud cover and precipitation, particularly in the ERA-40 dataset with respect to cloud cover (Chevallier et al. 2003; Dee et al. 2011; Kalnay et al. 1996; Uppala et al. 2005). Thus, while recognising that no single reanalysis dataset is perfect in its representation of the Earth's atmosphere both spatially and temporally, these reanalysis datasets represent the culmination of an enormous effort by the meteorological and climatological communities across the globe to accurately depict the state of the atmosphere since the mid-twentieth century.

The ERA-interim reanalysis product is currently publicly available free of charge at 0.75 ° latitude/longitude resolution (about 80 km at the horizontal scale), although it is worth noting that much higher resolution three- and two-dimensional data (e.g. EUMETSAT satellite data, polar-orbiting and limb-sounding satellites operating between 1 and 5 km horizontal resolution at nadir, weather balloons and aeroplane data) as well as other one-dimensional (e.g. weather station reports) have already been assimilated into the model using a state-of-the-art data assimilation procedure (Dee et al. 2011; Uppala et al. 2005). Unless explicitly stated, all reanalysis data used in this study are daily averages for the hours of 00, 06, 12 and 18UTC.

Later in the SASKYA project, it was decided to supplement the use of the reanalyses datasets with (near) real-time output from the much higher resolution UK Met Office Limited Area Model for Africa (Africa-LAM), kindly made available by the British Atmospheric Data Centre (BADC). This model has a grid box size of 12 km, meaning its 2-D horizontal resolution is some 50 times greater than that of ERA-interim—hence, it might be expected to show weather features relating to individual mountain ranges and large peaks, which could not be expected to be captured by the much coarser reanalysis product. More information on the Africa-LAM model is given in Section 3 of this paper.

1.5 The candidate sites

At the very start of the SASKYA project, basic topographical maps of Kenya were consulted in order to identify key mountain locations for a possible future telescope. Initially, ten candidate sites were chosen; the latitude and longitude coordinates and height above sea level of each of these candidate sites are listed in Table 1. Of these sites, four lay to west of the Rift Valley [highlighted by italics in Table 1; two of which lay at high altitudes above 3300 m (Mtelo and Cherangany Hills)]. The remainder (Table 1, numbered from 1 to 5) were to be found across a range of medium to high altitudes (~1300–2800 m) to the east of the Rift valley, with the only exception being a northern shoulder of Mount Kenya (referred to as "The Barrow"; see Table 1, number 10), where a possible site was identified at the very high altitude of 4417 m.

As the research progressed, however, it soon became apparent that two of the aforementioned sites (Loita hills and Kapcholio) were too moist (in terms of cloud cover and humidity, respectively; see Tables 2, 3 and 4) and therefore could be dropped from any further analyses. The Ndoto peak was immediately dropped from the list too, because of its relative close proximity (within 0.3 ° latitude/longitude) to

Table 1 The 13 initial candidate sites identified at the start of SASKYA

No.	Name	Latitude (° N)	Longitude (° E)	Altitude (m)
1	Mount Kulal	2.72	36.93	2293
2	Ol Donyo Nyiro	2.09	36.85	2752
3	Ndoto	1.75	37.17	2297
4	Mount Marsabit	2.28	37.95	1420
5	Warges	0.95	37.40	2688
6	*Kapcholio*	*2.12*	*35.15*	*2790*
7	*Loita Hills*	*−1.70*	*35.80*	*2642*
8	*Mtelo*	*1.39*	*35.21*	*3325*
9	*Cherangany hills*	*1.21*	*35.27*	*3369*
10	Mt. Kenya (The Barrow)	−0.09	37.19	4417
11	Ol Donyo Lenkiyo	1.45	37.09	2550
12	Un-named peak near Furroli	3.45	38.02	1869
13	Un-named peak near Sololo	3.36	38.39	1300

The latitude, longitude and altitude (m) of each site is given. Entries in italics are sites located west of the Rift Valley

the Ol Donyo Nyiro mountain (the reanalysis data would be unable to differentiate any variations of climate within this distance), and it was therefore assumed a priori that Ol Donyo Nyiro was the more favourable of the two peaks due to its higher altitude (having thus lower PWV). Furthermore, a closer inspection of the Kenyan terrain and vegetation (using Google Earth and other means) revealed three new mountain peaks in the vicinity of the best performing sites (namely Ol Donyo Lenkiyo and another two un-named peaks, numbered from 11 to 13, respectively, in Table 1), and it was decided to conduct analyses for these additional sites as well.

2 Results, analyses and discussion of ERA-interim data

2.1 Cloud cover

2.1.1 Total and integrated cloud cover

The total cloud cover (tcc) variable was extracted from the nearest gridpoint value of the ERA-interim reanalyses at the location of each SASKYA candidate site, for the period 1981–2010. In addition to this, another variable [total integrated cloud cover (TICC)] was later calculated for each site by integrating the monthly mean value of cloud cover (cc) for each of the 37 vertical levels (z) of the ERA-interim reanalysis model, as follows:

$$\mathrm{TICC} = \int_{z_1}^{z_{37}} \mathrm{cc} \cdot dz \tag{2}$$

The relationship between ERA-interim total cloud cover and integrated cloudiness might therefore be expected to be straightforward, as the latter initially appears to be a simple integration of the former. However, as shown in Figs. 3.1 and 3.2 of Graham (2008a), this is not always the case because varying amounts of overlapping cloud layers will increase the integrated cloudiness value more so than the total cloudiness (as the latter is considered as just a two-dimensional layer). This assumption can be tested for Kenya, and Fig. 2 presents a scatter diagram (with best-fit line plotted) of mean ERA-interim integrated cloudiness over all of the atmospheric layers against total cloud cover for 12 of the SASKYA candidate sites (with the exclusion of Mount Kenya site) for the period 1981–2010 inclusive. The corresponding r^2 value of the relationship between the two variables is 0.94 (statistically significant at the 99 % confidence interval). However, once

Table 2 Mean annual and standard deviation (of monthly means) of total cloud cover (tcc) for the candidate mountain sites, based ERA-interim reanalysis (1981–2010)

Name	Altitude (m)	Mean annual total cloud cover (%)	Standard deviation of monthly means (%)
Mount Kulal	2293	29.7	12.84
Ol Donyo Nyiro	2752	33.3	14.13
Mount Marsabit	1420	29.7	12.84
Warges	2688	33.3	14.13
Kapcholio	*2790*	*53.0*	*12.34*
Loita Hills	*2642*	*52.4*	*11.69*
Mtelo	*3325*	*53.0*	*12.34*
Cherangany hills	*3369*	*37.8*	*14.67*
Mt. Kenya (The Barrow)	4417	46.8	13.49
Ol Donyo Lenkiyo	2550	33.3	14.13
Un-named peak near Furroli	1869	44.0	13.35
Un-named peak near Sololo	1300	38.4	14.07
3350m_above_ODY[a]	3350	33.3	14.13

[a] The peak labelled "3350 m_above_ODY" is not an actual peak, but refers to an arbitrary height of 3350 m above sea level in vicinity of the present-day Ol Donyo Nyiro mountain (2752 m) for comparison purposes—see text for more details. Entries in italics are sites located west of the Rift Valley

Table 3 Same as Table 2, but for mean total integrated cloud cover

Name	Altitude (m)	Mean total integrated cloud cover (%)
Mount Kulal	2293	31.4
Ol Donyo Nyiro	2752	32.0
Mount Marsabit	1420	33.0
Warges	2688	32.2
Kapcholio	*2790*	*56.6*
Loita Hills	*2642*	*48.5*
Mtelo	*3325*	*53.2*
Cherangany hills	*3369*	*37.8*
Mt. Kenya (The Barrow)	4417	17.9
Ol Donyo Lenkiyo	2550	32.0
Un-named peak near Furroli	1869	45.6
Un-named peak near Sololo	1300	38.4
3350m_above_ODY	3350	30.1

See text for the definition and estimations of total integrated cloud cover (TICC), as defined in Eq. 2

the Mount Kenya data is included, the r^2 value drops to 0.70 (significant at the 95 % confidence level), underlining the decreasing validity of this assumption when using relatively coarse-grained reanalysis products in areas of mountainous topography.

Furthermore, it is important to note at this stage that any vertical integration of cloud cover through the atmosphere may also depend upon the opacity of the various cloud layers, which may vary with height, cloud composition, water droplet/ice crystal size distribution and density, air temperature and cloud thickness, with the additional caveat that an astronomical or meteorological observer on the ground views a "hemisphere" of sky, not a vertical profile (Graham 2008a).

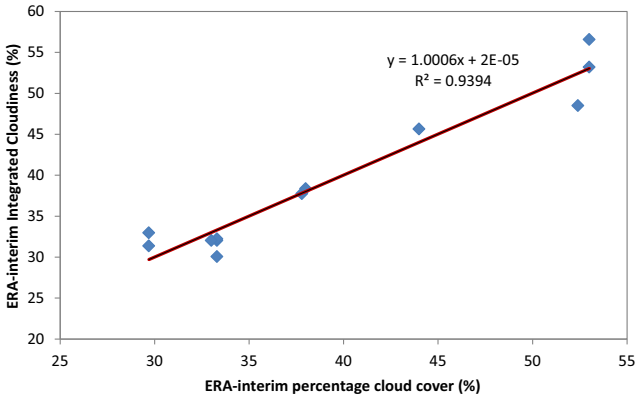

Fig. 2 Plot of mean ERA-interim (1981–2010) total integrated cloud cover (*TICC*) against total cloud cover (*tcc*), for 12 of the candidate SASKYA sites (excluding "The Barrow" site on Mount Kenya)

2.1.2 Maps and plots of total cloud cover for Kenya

Long-term (1981–2010) averages of ERA-interim total cloud cover for Kenya, and Hövmöller plots of cloud cover against altitude for the period January 2006 to December 2011 for all of the principal SASKYA candidate sites, are presented in Figs. 3 and 4, respectively. A summary of the average of these cloud cover conditions for each candidate site is also presented in tabular format in Table 2. Also presented in Table 3 are "total integrated cloud cover (TICC)" values for the same sites (as determined using Eq. 2).

Looking initially at Fig. 3a and b, these show the average annual total cloud cover at the 800 hPa (1500–2000m) and 600 hPa (~4000 m) levels, which encompasses the altitude range that we would expect the final telescope to be built at. These two images are contrasting; at 800 hPa, cloud cover is greatest over the east and south of the country, with a

Table 4 As Table 2, but for mean annual average and standard deviation (of monthly means) of precipitable water vapour (PWV)

Name	Altitude (m)	Mean annual PWV (mm)	Standard deviation PWV of monthly means (mm)
Mount Kulal	2293	14.5	2.4
Ol Donyo Nyiro	2752	10.7	2.3
Mount Marsabit	1420	23.0	3.0
Warges	2688	11.1	2.4
Kapcholio	*2790*	*14.1*	*2.0*
Loita Hills	*2642*	*14.7*	*1.7*
Mtelo	*3325*	*10.2*	*1.5*
Cherangany hills	*3369*	*8.5*	*1.7*
Mt. Kenya (The Barrow)	4417	3.7	1.1
Ol Donyo Lenkiyo	2550	12.4	2.4
Un-named peak near Furroli	1869	21.1	2.9
Un-named peak near Sololo	1300	24.1	3.3
3350m_above_ODY[a]	3350[a]	7.5	1.9

[a] The peak labelled "3350 m_above_ODY" is not an actual peak, but refers to an arbitrary height of 3350 m above sea level in vicinity of the present-day Ol Donyo Nyiro mountain (2752 m) for comparison purposes—see text for more details. Entries in italics are sites located west of the Rift Valley

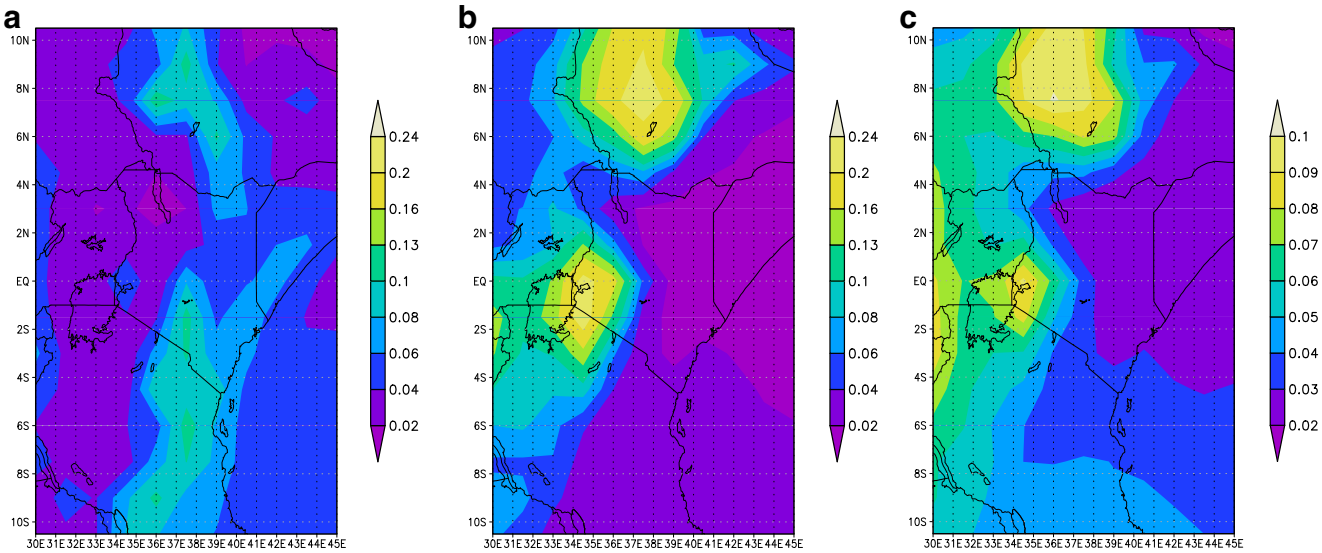

Fig. 3 Mean annual ERA-interim (1981–2010) cloud cover for **a** 800 hPa, **b** 600 hPa, and **c** average of 750 to 50 hPa

maximum near the (lower) slopes of Mount Kenya (and near its sister peak Mount Kilimanjaro, just across the border in Tanzania). This cloud is likely to be "warm" low-level stratocumulus or stratus cloud, which is most prevalent near the eastern coast of Kenya and it capped by a stable inversion at low levels. This is confirmed by Fig. 3b, which shows a

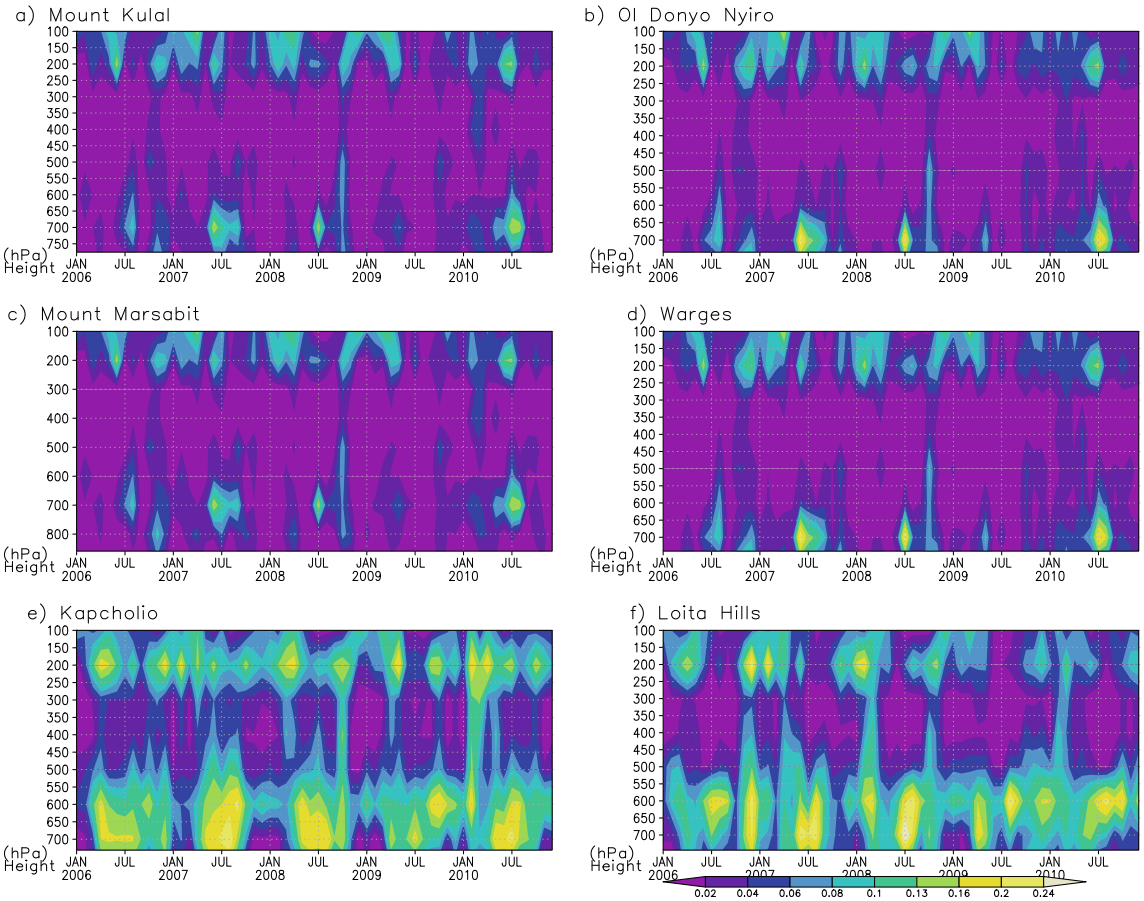

Fig. 4 **a**–**l** Hövmöller diagrams of ERA-interim cloud cover (*shaded colours*, fraction of sky covered), plotted with height (hPa) against time for 5 years from January 2006 through to December 2010, for the SASK YA candidate sites. Height (altitude) above each candidate site is plotted on the *Y*-axis (hPa)

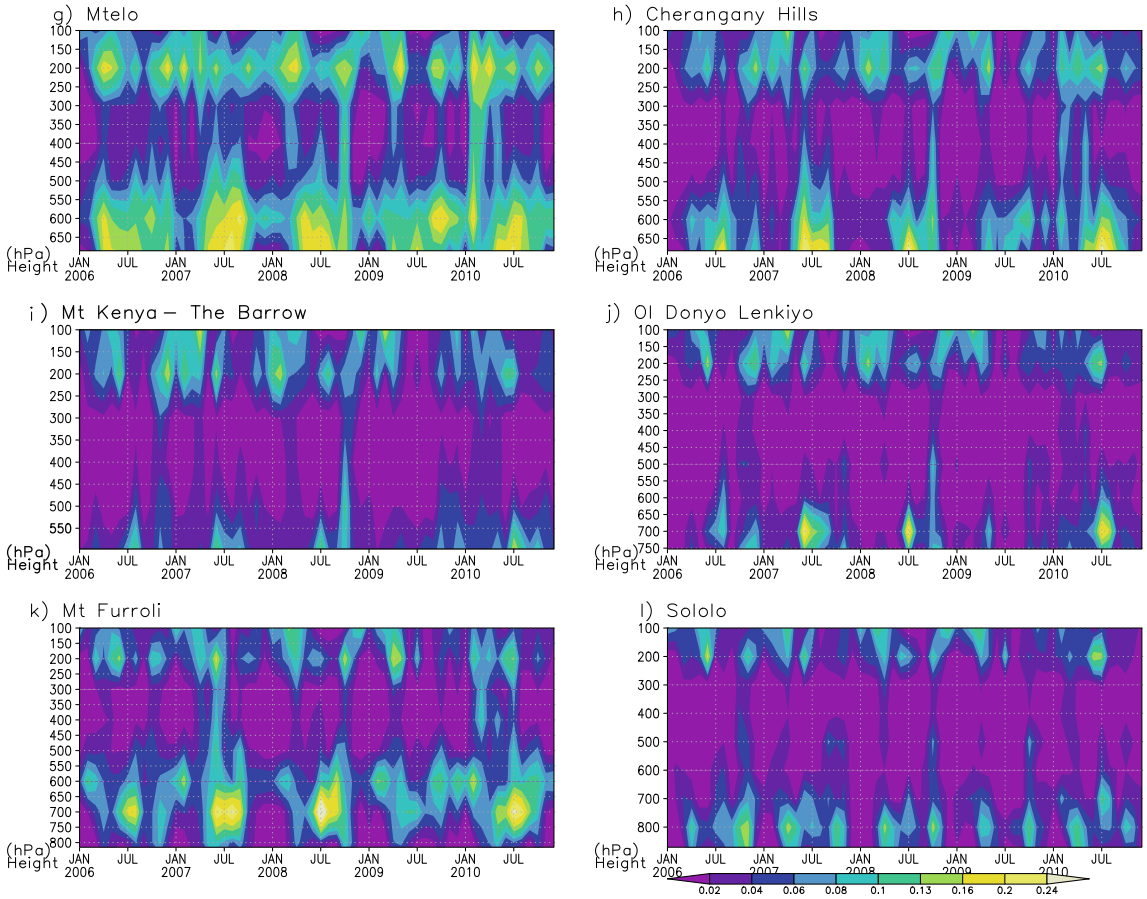

Fig. 4 (continued)

near complete absence of cloud across the east and northeast of the country at the 600 hPa level, but clearly shows a tendency towards increased cloud cover over the southwest of Kenya, most especially near to the eastern shoreline of Lake Victoria. As stated earlier, diurnal lake-breeze air circulation systems in this region give rise to frequent and powerful thunderstorms lasting into the night hours (Lumb 1970; Yin et al. 2000), and this seems to be reflected in the cloud statistics for this region.

When the cloud cover data at all levels from 750 to 50 hPa are averaged (this latter height corresponds to an altitude of approximately 25 km in the stratosphere, well above even the highest clouds at this tropical latitude), the result (Fig. 3c) confirms a general southwest to northeast decreasing gradient in cloud cover across Kenya. Using the altitude range from 750 to 50 hPa in this instance is more or less equivalent to integrating the bulk cloud fraction for each atmospheric layer from a height of approximately 2500 m upwards. In other words, we are trying to graphically present a value that is equivalent as close as possible to the mean annual percentage cloud cover that would be reported by an observer at an astronomical observatory at an altitude of 2500 m anywhere in Kenya.

A second cloudier region in southern Ethiopia, north of the Lake Turkana, is also evident in all three of these maps, which may have implications for the two un-named SASKYA candidate peaks near Furroli and Sololo (sites labelled 12 and 13 as listed in Table 1).

An additional imaginary site (indicated by a superscript letter a in Table 2, and referred to as "3350m_above_ODY"), referring to an arbitrary height of 3350 m above sea level in the vicinity of Ol Donyo Nyiro mountain, was also included, for the purpose of making "like-for-like" comparisons between the east and west sides of the Rift Valley (as stated earlier, the mountain summits on the west side of the Rift Valley reach as high as this altitude, but those on the east side do not).

Meanwhile, the Hövmöller plots of cloud cover with altitude from January 2006 to December 2010 (inclusive) are presented in Fig. 4a–l. These images provide, at a glance, the temporal and spatial evolution of cloudiness at each selected candidate site over a period of 5 years of recent climatological history. It is immediately apparent from these sub-figures that all sites east of the Rift Valley are less cloudy than those west and south of the valley (for example, compare Mount Kulal, Ol Donyo Nyiro and Warges, with Kapcholio, Loita Hills and Mtelo). Also immediately discernible, at all sites, is the prevalence of two layers of cloud (the first lower layer averaging from

approximately 700–550 hPa, and the second upper layer averaging from 250 to 100 hPa).

This latter cloud layer (from approximately 250 to 100 hPa) is common to all of the candidate Kenyan sites. This presumably is cirrus ice cloud, and may be the remnants of thunderstorm anvils drifting away eastwards from the Lake Victoria region, and remaining suspended high in the atmosphere for many hours after the dissipation of the original storms that produced them. These could pose significant problems for night-time astronomical observation in Kenya, and any ground observation or site testing study would need to closely monitor the occurrence and frequency of such clouds and the degree of extinction they pose.

The least cloudy candidate sites, according to the ERA Interim reanalysis data based on the 30-year period from 1981 to 2010, are Mount Kulal and Mount Marsabit (Fig. 4a, c; Table 2) with a mean annual cloud cover values of 29.7 % apiece. This is slightly less than the mean annual value of 33.3 % determined for Ol Donyo Nyiro and Warges. The value for the "The Barrow" site on the northern shoulder of Mount Kenya (4,417 m) is 46.8 % (Table 2); however, it is important to note that local orographic cloud formations over the mountain will hardly be resolved by the reanalyses at this scale (a relatively coarse resolution of 75 km).

The decrease in cloud cover across Kenya as one moves north is apparent when one considers that the value obtained on the high shoulder of Mount Kenya (4417 m) can be easily achieved at the much lower altitudes (below 3000 m) on summits further north, such as Ol Donyo Nyiro (see Table 2). Meanwhile, the values for Mtelo and Kapcholio are very high (both 53.0 %), but are not surprising for locations west of the Rift valley, for the reasons as already discussed. Surprisingly, the relatively low summits of (un-named peaks near Furroli and Sololo, respectively) are cloudier than Mount Kulal, possibly due to influence from the Ethiopian cloudy area to the north of the Kenyan–Ethiopian border, as mentioned earlier.

Thus, in order to put these cloud statistics into full perspective from an astroclimatological viewpoint, the total cloud data fractions of just <30 % obtained at Mount Kulal and Mount Marsabit are almost equivalent with values from, e.g. Maidanak observatory in Uzbekistan (Ehgamberdiev et al. 2000; as stated earlier). At the same time, they cannot realistically compete with premier sites such as San Pedro Mártir in Mexico (Tapia 1992) or the Chilean sites of Paranal or La Silla (ESO 2015).

Another main feature of the cloud data shown in Figs. 3 and 4 is the high degree of seasonal and inter-annual variability—this is to be expected in Kenya, where not only are there large changes in weather associated the monsoon twice a year, but the monsoons themselves can vary in intensity significantly from year to year and from decade to decade (Nicholson 1996). Strong links between the El Niño Southern Oscillation (ENSO) global climate phenomenon are known to occur (Marchant et al. 2007), with generally increased precipitation in El Niño years, and correspondingly weaker monsoons or droughts in La Niña years.

Perhaps surprisingly, diurnal variations in cloudiness do not appear to be large in Kenya. Initial studies using the *FriOWL* software (Graham 2008a) show that the only part of Kenya with a significant variation in daytime/night-time cloudiness is the region near Mount Kenya (with a variation of the order of 40 %, not shown).

Finally, it is important to note that all reanalyses cloud data has a higher degree of uncertainty (or a lower level of confidence) than for other meteorological variables such as air temperature, humidity or wind, as detailed by Chevallier et al. (2003). However, we may expect better quality cloud data in Kenya than in mid-latitude regions, as the assimilated EUMETSAT satellite data has highest resolution nearest the equator (as the satellite is at nadir), and there should be a good contrast in the temperature between cloud and land in Kenya (through which algorithms are used to determine if a cloud exists or not, based on satellite imagery).

2.2 Precipitable water vapour

Precipitable water vapour (PWV) is an integrated value for the total humidity of the atmospheric column, and can be thought of in the most simplistic sense as "the depth of water around your ankles, should all the water vapour in the atmospheric column above your head be precipitated into liquid water in a single instant" (Graham 2008a). In order to calculate PWV from the topographic surface upwards (as PWV decreases rapidly with height), partial PWV integrations [p(PWV)] from the height of each individual mountain peak (Table 1) to the effective top of the atmosphere were calculated using thirty years of data (1981–2010) from the ERA-interim reanalysis model data, as follows:

$$p(\mathrm{PWV}) = \int_{Z_1}^{Z_{37}} q \cdot \, \mathrm{d}z \tag{3}$$

where q is the specific humidity of each layer (dz) of the model above mountain height.

Table 4 lists the mean annual average partial PWV and standard deviation (of monthly means) for all of the candidate sites, based on 30 years of climate reanalysis model data from 1981 to 2010. With the exception of The Barrow candidate site on Mount Kenya, mean annual precipitable water vapour (PWV) values, as determined by the reanalyses, are higher than the previously mentioned threshold of 5 mm for satisfactory operation of telescopes at visible wavelengths for all sites (Sarazin 2003, personal communication).

Meanwhile, in an attempt to indicate the considerable seasonal and inter-annual variability of PWV in the region,

Fig. 5a–i depicts the relationship between specific humidity and height (in hPa) for all of the remaining candidate sites, plotted against time for the period January 2006 until December 2010, using the ERA-interim reanalyses model data. Here, the vertical integral of the specific humidity from the land surface to the top of the atmosphere is the same as the

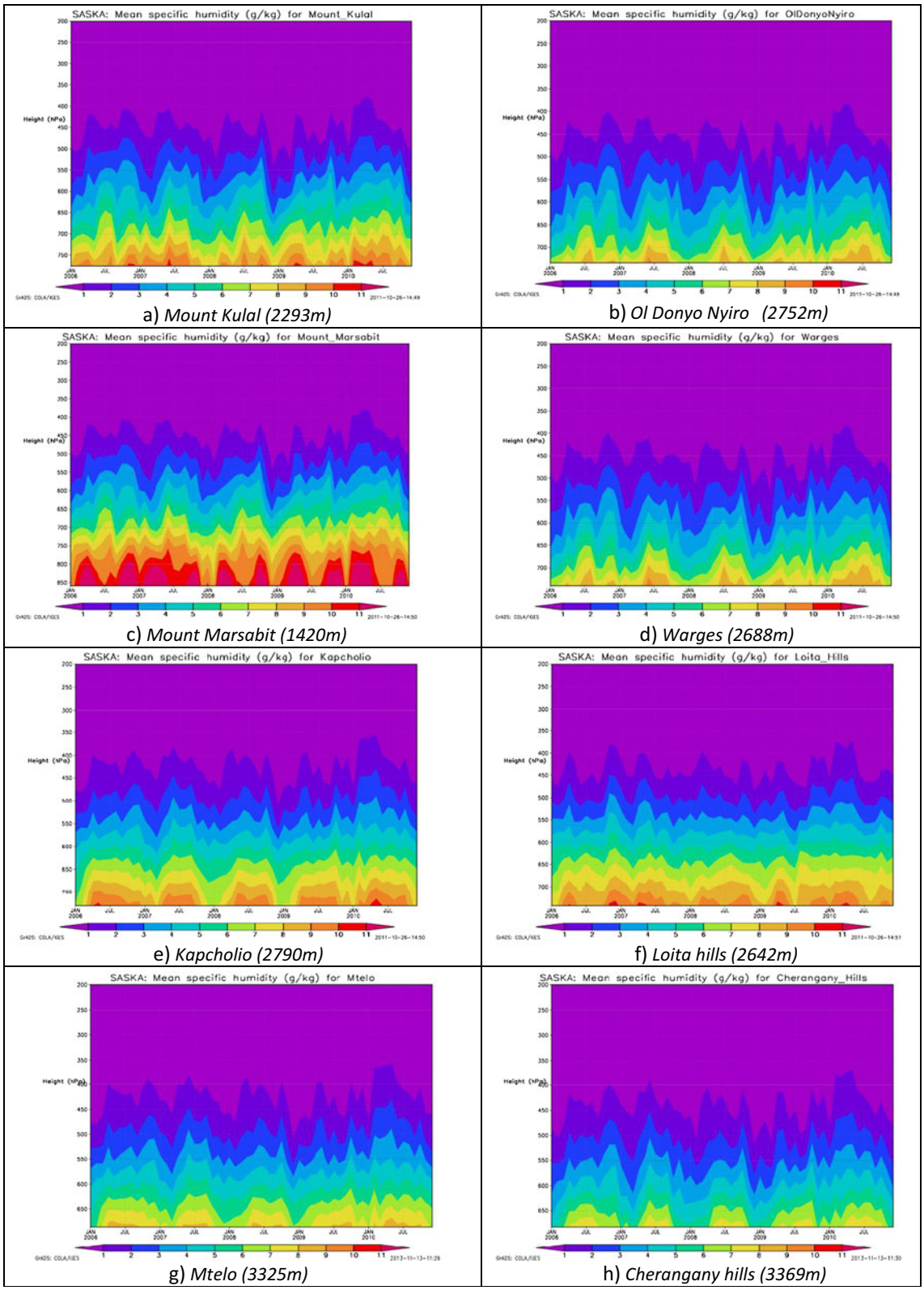

Fig. 5 **a**–**l** Same as Fig. 4, but for specific humidity [*shaded colours*, g/kg (grams of water per kilogram of air)]

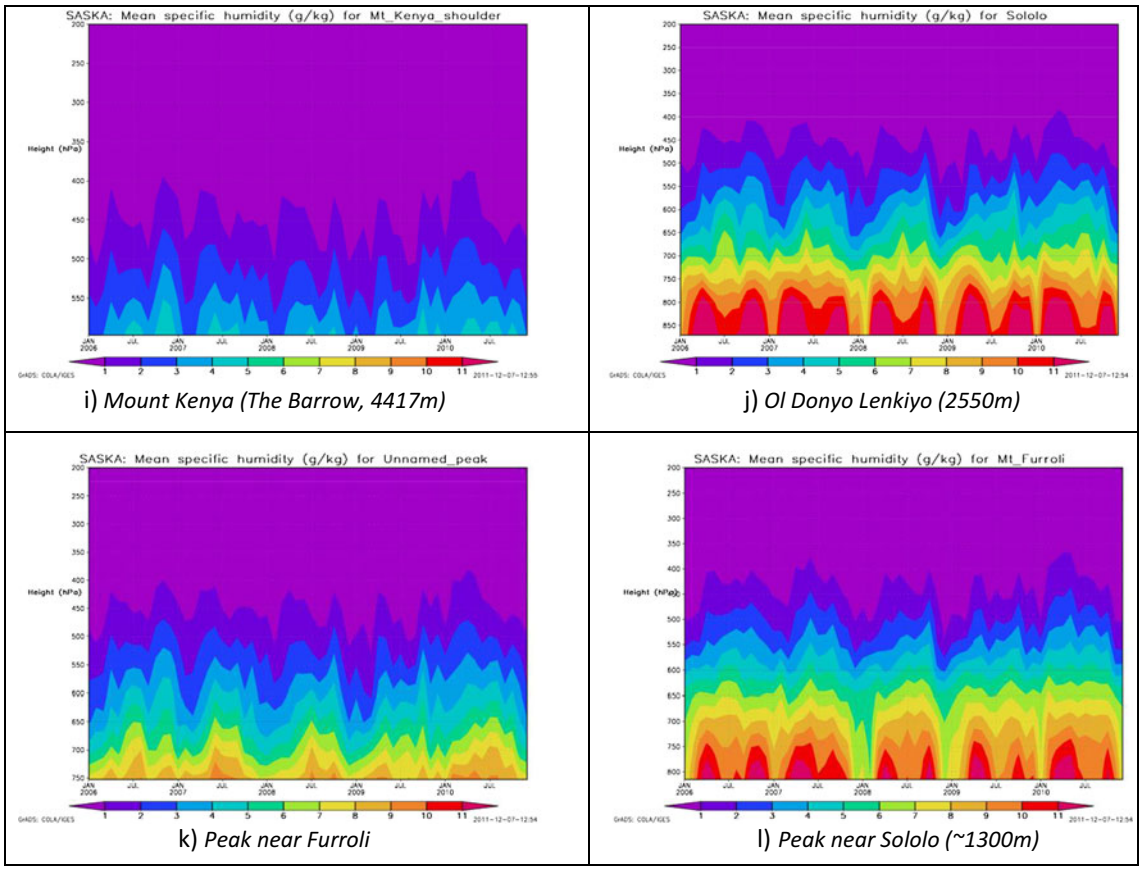

Fig. 5 (continued)

PWV (Eq. 3). The units of specific humidity are grams of water per kilogram of air, and so the lower the amount of water vapour above each site, the lower the final PWV value will be.

By visually comparing Fig. 5a–i against one another, it can be seen that Ol Donyo Nyiro, Cherangany hills, Mtelo, Warges and especially Mount Kenya [not the actual summit of Mount Kenya, but a candidate site (The Barrow) on the northern shoulder of the mountain at 4417 m, as stated earlier] have the lowest amounts of specific humidity above their summits throughout the year, in agreement with the PWV values presented in Table 4. This is not surprising as they are the highest sites; as stated earlier, the water vapour content of the atmosphere at any place is highly dependent on altitude.

Other reasonably well-performing sites are Ol Donyo Lenkiyo (east side of the Rift Valley), Mtelo and Cherangany hills (west side of the Rift valley); these latter two sites are at altitudes of 3325 and 3369 m, respectively. However, when the imaginary site (labelled as "3350m_above_ODY" in Table 4) to the east of the Rift Valley is considered [i.e. at the same height at Mtelo/Cherangany hills (~3350 m) but at the same geographical co-ordinates as Ol Donyo Nyiro), we see that the mean PWV is considerably lower (7.5 mm) than that to the west of the Rift Valley. In other words, Mtelo mountain has a mean PWV of 10.2 mm, about the same as Ol Donyo Nyiro (10.7 mm), despite the former being 600 m higher in altitude than the latter. Similarly, the value for the Cherangany hills (3369 m) is 8.5 mm, but above Ol Donyo Nyiro (extrapolated to a height of 3350 m), the equivalent PWV is only 7.5 mm. Therefore, an obvious first conclusion is that lower PWV values are to be found on the east side of the Rift valley. This is an important finding, as it more or less leads us to exclude all peaks west of the Rift Valley from our study, for we can ascend to a lower height on the East side, yet still attain levels of PWV comparable to a much higher site on the west of the valley.

The frequency distribution of PWV for a selection of six of the candidate sites can be seen in the plotted histograms of night-time data for at each of six of main candidate sites in Fig. 6a–f. The datasets were not tested for normality, but the shapes of the various distributions in Fig. 3 suggest the PWV data (expressed as monthly means) are distributed in an approximately normal fashion, with the exception of the Mount Kenya site and the un-named Peak near Sololo (the highest and lowest sites, respectively). The frequency distributions also enable us to determine the temporal probability of a certain PWV threshold being crossed—a quick glance at the histograms confirms that Mount Kenya is the only site where PWV values of lower than 5 mm could be expected to be routinely observed. The frequency distribution histograms also show that Ol Donyo Nyiro records a PWV of below

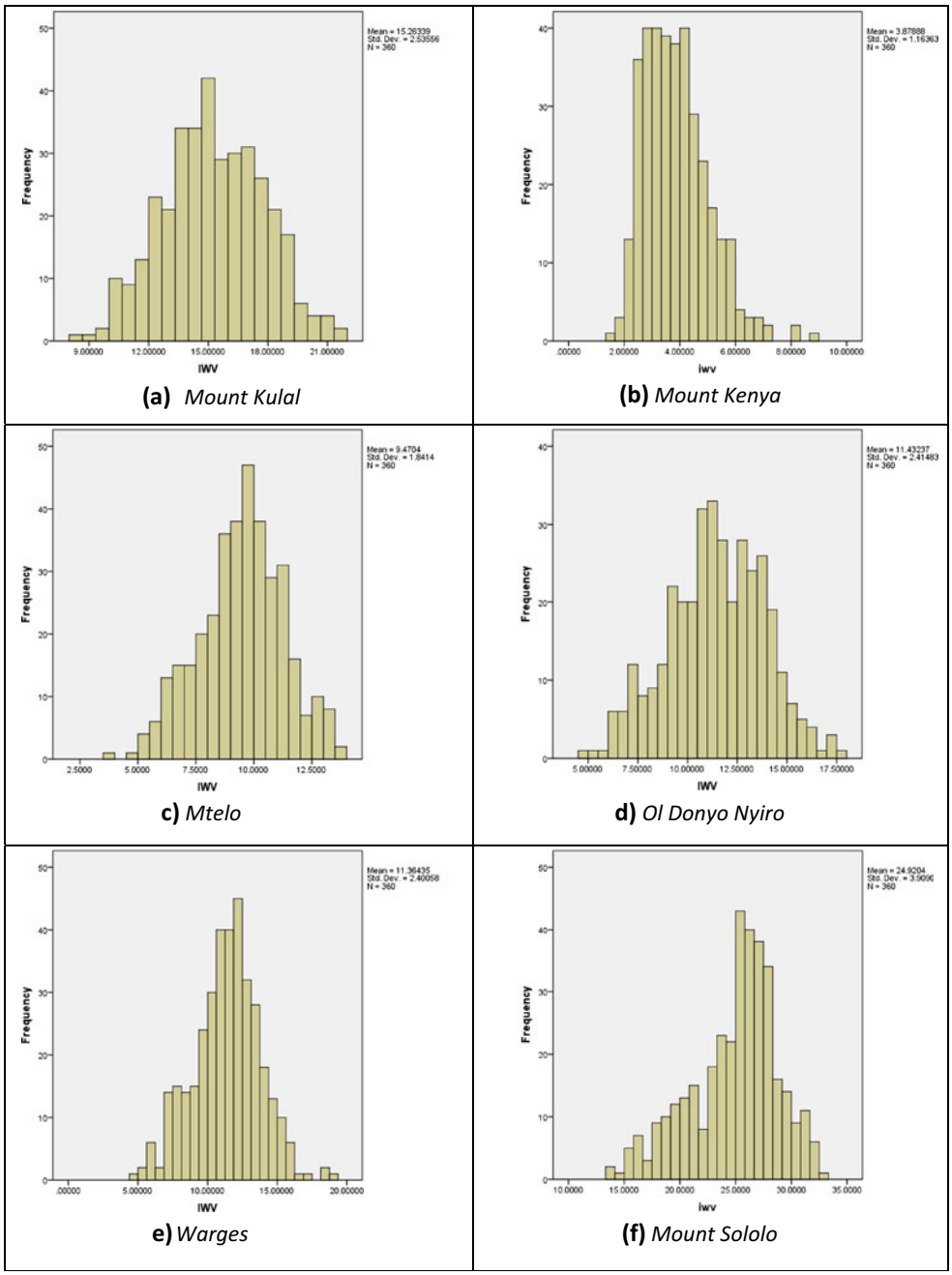

Fig. 6 **a**–**f** Frequency distribution histograms of mean monthly (1981–2010) ERA-interim integrated water vapour (*IWV*, the same as PWV) for six of the candidate sites

5 mm on <1 % of days per year. Over the Cherangany hills, values of 5 mm are also reached for approximately 1 month/year (8 % of days), but at the same altitude (site "3350m_ODY") to the east of the Rift valley, the threshold is reached for approximately 2 months of the year (17 % of days per year).

A study of night-time only data (ERA-interim, 1981–2010) also showed no significant differences in PWV between daytime and night-time across the whole range of candidate sites, with night-time values typically lying within ±0.5 mm of daily values, or less. Variability in smaller amounts and on smaller scales cannot be resolved by the reanalyses—this could be determined using higher resolution meteorological model data (see the following section on the UK Met Office Africa-LAM model).

Finally, a three-dimensional plot of the average height of the 1981–2010 ERA-interim PWV 5 mm "surface" across Kenya (Fig. 7) shows that it decreases in height from the northwest towards the southeast of the country (the 5 mm PWV "surface" is the height one would need to go in the atmosphere above Kenya to reach an annual long-term average PWV value of 5 mm). This surface, sloping to the southeast, is incised

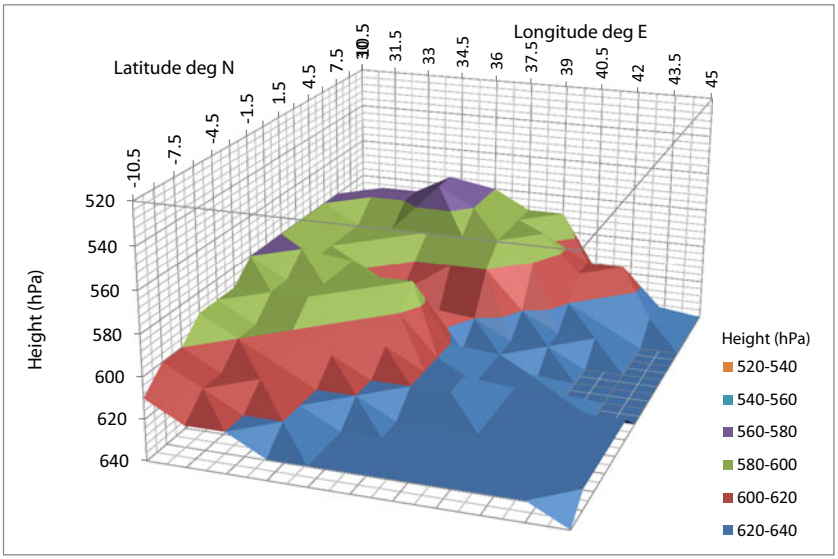

Fig. 7 A schematic depiction of the height of the average (1981–2010) ERA-interim 5 mm precipitable water vapour (PWV) surface over East Africa. Longitude and latitude are plotted on the *X*- and *Y*-axes, respectively, with height (hPa) plotted on the *Z*-axis

by a narrow region of lower 5 mm PWV surface heights, which corresponds directly with the Rift valley. Overall, one must ascend to an approximate altitude of about 580 hPa (~4500 m, near the freezing level) in north-west Kenya to intercept the mean annual 5 mm PWV surface, but only to 620 hPa (nearer ~4000 m) in the southeastern part of Kenya. Interestingly, this PWV gradient lies at a right angle to the average cloud cover gradient identified earlier in the preceding section (Fig. 3c). This confirms that PWV in Kenya is not necessarily related to cloud cover or precipitation, as has been confirmed by other studies (e.g. Koffi et al. 2013). It just so happens that PWV is converted into cloud and precipitation more efficiently in the southwest of the country than elsewhere.

2.3 Vertical velocity variable (*w*)

Graham (2008a) discovered that areas of gently descending air across a large area, identified using the ERA-40 reanalysis (Uppala et al. 2005), qualitatively correlate well with the locations of the most well-established astronomical observatories (e.g. the Canaries, Chile, southwestern Africa, southwestern USA and Mexico). The reason for the correlation is because gently descending air is often associated with stable air masses (i.e. high pressure, a low amount of turbulence and adiabatic warming through descent, which leads to stable inversions). In these situations, thermal turbulence due to instability (the main cause of poor seeing conditions) is at a minimum. The vertical velocity (*w*), when understood in the case of gently subsiding and adiabatically warming air, can therefore be used as a good proxy for atmospheric stability, and hence good astronomical seeing (positive values of *w* mean a downward flow of air towards the ground, and vice versa).

Figures 8a and b presents the mean annual vertical velocity (Pa/s) for all atmospheric layers from (a) 750 to 50 hPa and (b) 600 to 50 hPa, respectively. Figure 8a clearly shows the most favourable conditions (gently subsiding air) located in a region stretching from Mount Kulal, across the Chalbi desert and towards the Ethiopian border. At the same time, moderately favourable values are still to be found across most of Kenya east of the Rift valley, even as far south as Mount Kenya.

Meanwhile, Fig. 9a–f shows the 2006–2010 time series of the vertical velocity variable for six of the selected candidate sites. The contrasts between Fig. 9a, Mount Kulal (mostly gently descending air), and Fig. 9e, Kapcholio (large parts of each year with ascending motions of air), are clearly apparent. All candidate sites show significant seasonal variation of vertical velocity, however, and this would impose a significant constraint on the timing/seasonal planning of astronomical observations. Furthermore, there appears to a deep surface boundary layer (a region of turbulent air near the surface) above several candidate sites (Fig. 9a–f), reaching above 700 hPa (~3000 m), but it may be much shallower by night. This would need to be investigated in greater detail by any site selection team on the ground and a closer inspection of night-time only data.

2.4 Relative humidity

High night-time relative humidity (rh) can be detrimental for astronomical observation due to the possible collection of dew or frost on the telescope mirrors or lenses, leading to distortion of the stellar image as well as being problematic for the successful operation of optical equipment. In this respect, large telescopes today are usually sited within, or near the

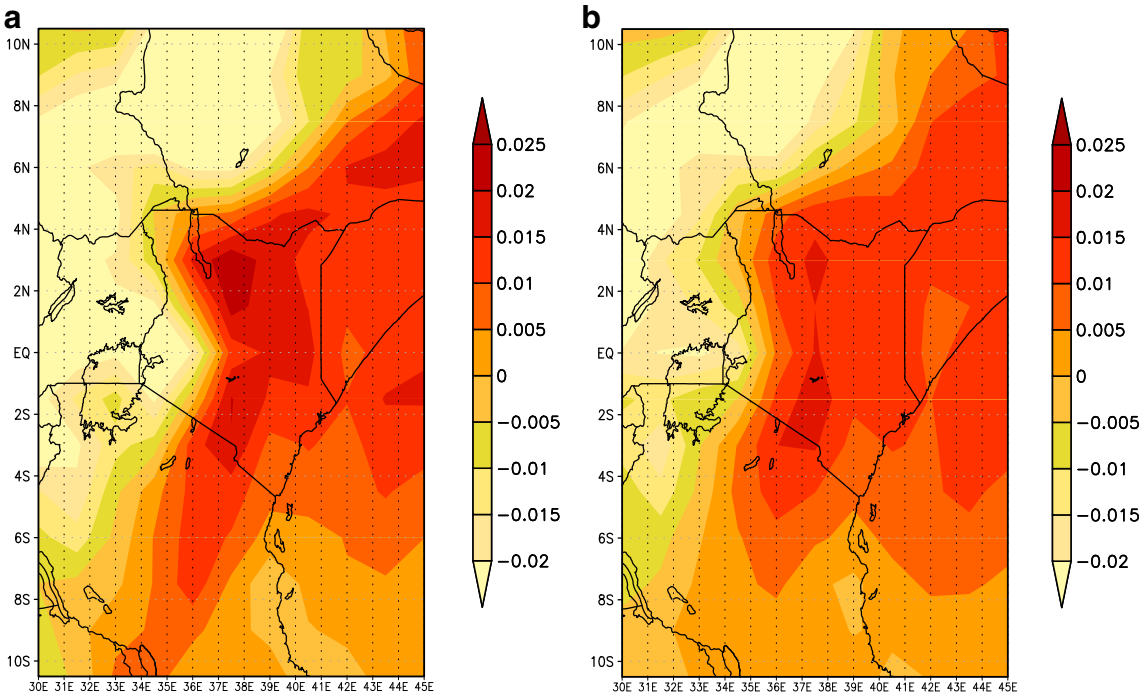

Fig. 8 **a** Mean annual 1981–2010 ERA-interim vertical velocity (*w*, Pa/s) from 750 to 50 hPa and **b** from 600 to 50 hPa

borders of desert area and where moisture sources are kept at a minimum. It is perhaps an inconvenience for astronomers that the highest relative humidity usually occurs at night-time; this is a consequence of the diurnal pattern of air temperature at the surface of the Earth and the strong relationship between air temperature and relative humidity.

Figure 10 shows the long-term patterns of relative humidity (rh) with height for six of the main candidate sites, as described earlier. High relative humidity (>65 %) occurs at all sites close to the ground and up to a height of approximately 700 hPa (~3,000 m); this is probably caused by a deep turbulent boundary layer in Kenya, advecting moisture to a significant height (>3,000 m), as mentioned earlier. An area of low rh (<40 %) is apparent from approximately 700 to 250 hPa, but there is a second area of high rh between 250 and 50 hPa (>10,000 m) at all sites—this is probably related to the high incidence of cirrus cloud, as noted earlier. There is also strong seasonal and inter-annual variation of rh, however. (Note the unique "spike" in the middle of each subplot—due to the intense El Nino event of 1998).

The objective for SASKYA would be to find a site that lies within the band of reasonably low relative humidity between 700 and 250 hPa; at present, all sites excepting Mount Kenya do not attain this level, at least according to the meteorological model data.

2.5 Wind speed

Sarazin (2003) quotes an ideal steady wind speed at a large astronomical observatory to be in the range approximately 2–8 m/s (4–16 knots; 7–29 km/h), although some modern observatories can operate up to wind speeds of 14 m/s when observing downwind (with shelter provided by the dome). Too low wind speeds affect astronomical observation by incomplete flushing of the telescope enclosure leading to what is known as thermal "dome" seeing, whereas too high wind speeds can cause shaking.

Figure 11 shows the average annual (1981–2010) ERA-interim prevailing wind vectors above Kenya at the 700 hPa level, which is the approximate height at which an observatory is hoped to be constructed in Kenya. The predominant winds are northeasterly, between 2 and 5 knots (1–3 m/s; 4–9 km/h) in velocity. These speeds are at the lower end of Sarazin's (2003) categorisation, but local accelerations can be expected near the summit of peaks. On the other hand, the risk of strong winds seem to be less likely. Further studies of local winds would be necessary once a candidate site has been established in order to determine the best possible exact location for a telescope.

2.6 Aerosols and dust contamination

As stated earlier, high aerosol or dust loadings are problematic for the successful operation of telescopes and optical equipment in arid or semi-arid regions, as they can interfere with the optical mechanisms in telescopes, degrade mirrors by "sand-blasting" and they also increase the extinction of light on its path through the atmosphere (Giordano and Sarazin 1994; Siher et al. 2004).

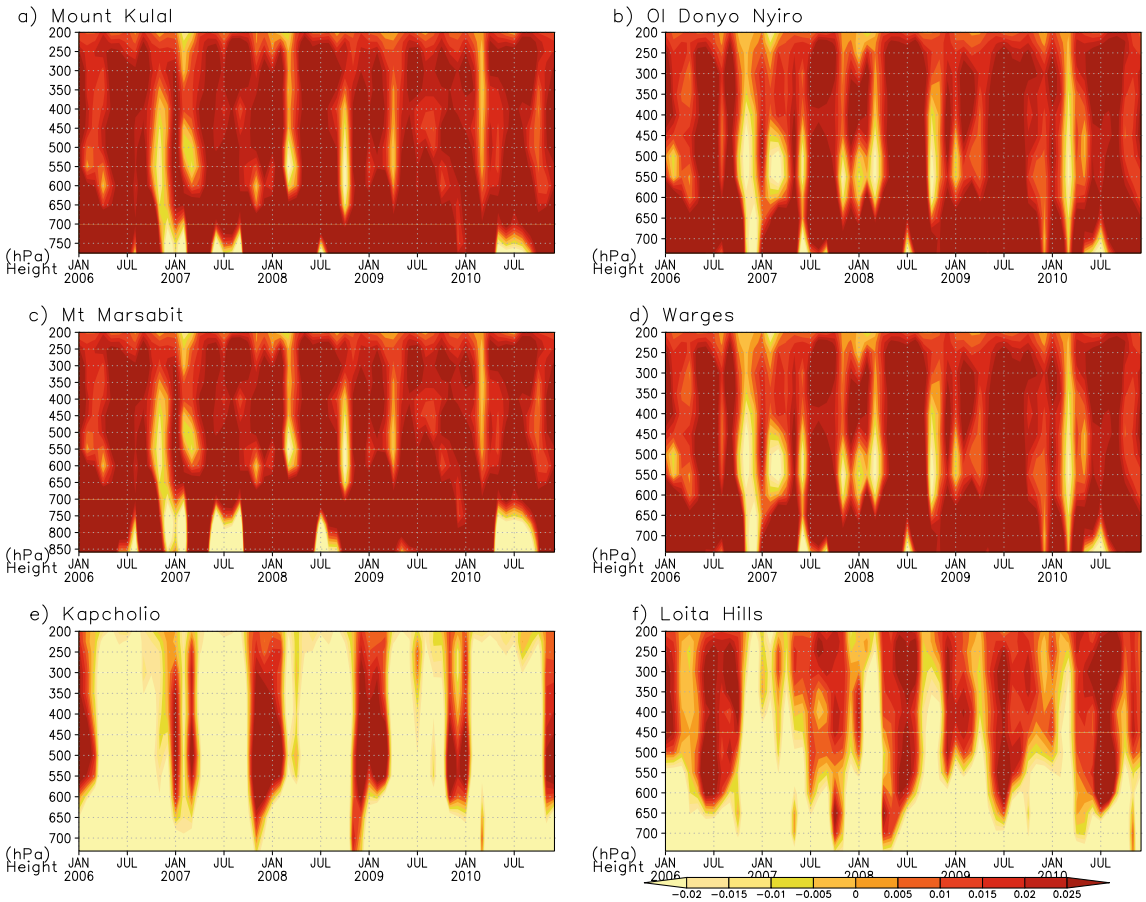

Fig. 9 **a**–**f** Same as Fig. 4, but for vertical velocity (Pa/s), for the six selected candidate sites, as labelled

Figure 12 shows the maximum TOMS aerosol index recorded during the 21-year period from 1981 to 2002 for the whole of the East Africa and western Indian Ocean region (see Graham 2008a, for a fuller explanation of the TOMS algorithm). It confirms that Kenya is fairly well protected from most of the sources of atmospheric dust and aerosols in Africa, namely desert dust blown from the Sahara and fine aerosols due to biomass burning in central Africa.

3 Overview of UK Met Office high-resolution African Limited Area Model data used

Following completion of the first part of this study using the ERA-interim reanalysis dataset, as outlined in the previous section, high-resolution meteorological data from an operational model for Africa became available for the first time. As part of a major technical co-operation project in numerical weather prediction for Africa, the UK Met Office (UKMO) made available their Africa Limited Area Model (Africa-LAM) to academic researchers for the period 2010–2013 (UKMO 2012). The availability of high-resolution operational model data represented a new opportunity for us to examine the regional, and possibly even local, characteristics of the weather and climate across the Kenyan Highlands that hitherto had been impossible due to the relatively coarse resolution of the reanalyses datasets.

3.1 Specific details of the UKMO Africa-LAM with regards to SASKYA project

The UKMO Africa-LAM is a “non-hydrostatic” meteorological model, meaning that hydrostatic balance in the Earth’s atmosphere is not always assumed (UKMO 2012). Thus, the model may permit the formation of non-geostrophic mesoscale meteorological phenomena, such as local mountain-valley winds or lake breezes, in certain situations. Full prognostic equations with no approximations are used in two different configurations of the model, the first with 38 vertical levels (L38) and second with 70 vertical levels (L70) (UKMO 2012). Output from the L70 model was used only in this study. The horizontal grid resolution of the L70 configuration is 12 km, and the horizontal extent of the model stretches from the Atlantic Ocean (22 ° W) to the Indian Ocean (62 ° E) and

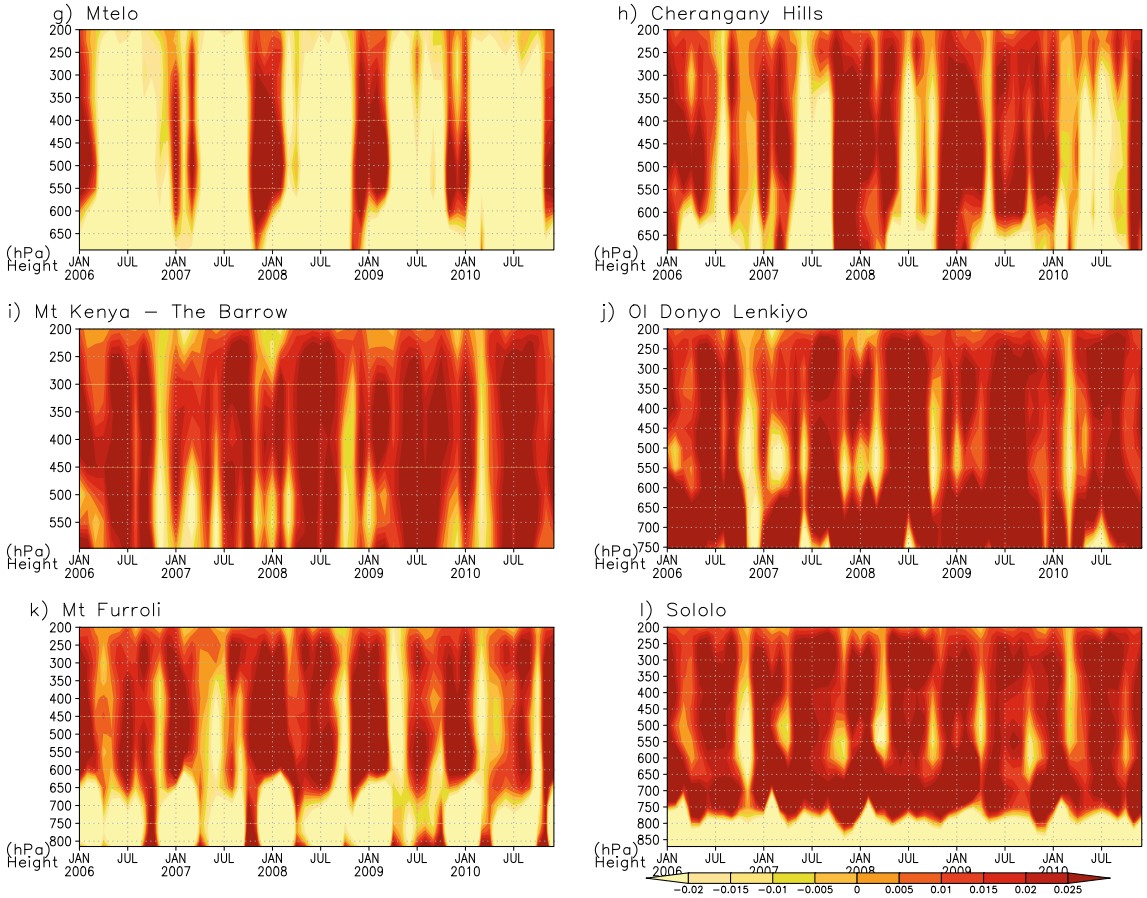

Fig. 9 (continued)

from central Africa (10 ° S) to just north (45 ° N) of the Mediterranean Sea (UKMO 2012).

The Africa-LAM was run by the UKMO three times per day at the times of 06z, 12z and 18z. Output from the 18z run was used only in this work because the 18z run performed a new data assimilation method. This is where observational data are interpolated onto the model grid as accurately as possible, minimising errors, using meteorological output from the previous cycle as the background fields. The boundary conditions of the model were set to the UKMO global model (UKMO 2012).

The Africa-LAM differs from the reanalyses datasets such as ERA-interim (Dee et al. 2011), ERA-40 (Uppala et al. 2005) and NCEP-NCAR (Kalnay et al. 1996) both in terms of data assimilation and the type of meteorological model used. The Africa-LAM output is merely a forecast, but reanalyses are a combination of a tried-and-tested state-of-the-art meteorological model with a fully comprehensive data assimilation scheme. The Africa-LAM certainly has significantly much greater resolution than most reanalyses (at 12 km, the horizontal grid resolution of the Africa-LAM L70 is 10^2 times greater than those of most reanalyses), but unlike the reanalyses, the Africa-LAM may not be fully validated in all meteorological situations and therefore may not accurately capture all meteorological phenomena within its domain. Indeed, the UKMO ceased to run the Africa-LAM from mid-2013 onwards, as it was being out-performed by the UKMO global model, even when the latter model was run at a coarser resolution (UKMO, 2013, personal communication). A further disadvantage in using an operational model such as Africa-LAM in comparison to the ERA-interim reanalysis is the fact that the former has a much shorter temporal data archive (in the case of the of the Africa-LAM, it is <3 years, compared to almost 35 years of archived data for ERA-interim, and even longer for other reanalyses such as ERA-40 and NCEP-NCAR). This final point is important from a climatological point of view for Kenya because the tropics typically have large and significant inter-annual and inter-decadal climatic variability.

Owing to the large size of the Africa-LAM domain (approximately 20 million km^2), the high vertical resolution of the model (L70, 12 km) and the high number of prognostic variables (over 50), a significant drawback to its ease of use became apparent during SASKYA, as the amount of

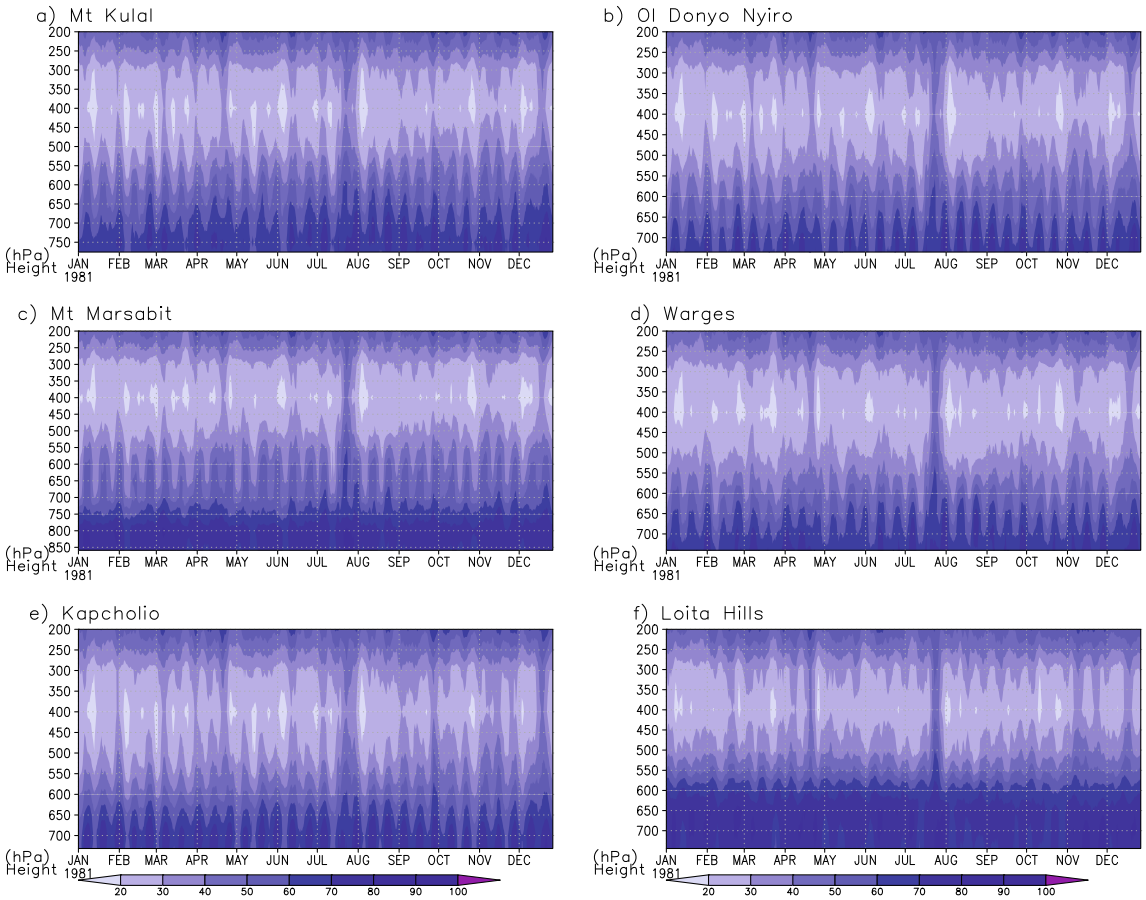

Fig. 10 **a**–**f** Same as Fig. 9, but for relative humidity (%)

electronic data to be downloaded from the British Atmospheric Data Centre (BADC; where output from the UK Met Office Africa-LAM is stored online) was very large, both in terms of download time and storage costs. Even for a single model run, the data amounted to more than 10^9 bytes (gigabyte) of information. This problem arose because it was only possible to download all meteorological variables for complete domain of the Africa-LAM as a single UK Met Office binary file ("*PP*" formatted) for each model run, rather than as a subset of the original large data files.

Thus, in order to keep the relatively small SASKYA project within scope and budget, only a limited amount of output data from the Africa-LAM could be downloaded and analysed in this study. It was therefore decided to concentrate solely on the two most important meteorological parameters, which would affect the potential suitability of each site for future astronomical observation, namely (i) cloud cover and (ii) specific humidity (i.e. PWV). It was also decided to limit the study of these variables to the following four best-performing SASKYA candidate sites, namely:

1. Warges
2. Mount Kulal
3. Ol Donyo Nyiro
4. Mount Kenya (The Barrow).

Output data from the Africa-LAM was then downloaded for 33 different instances of the model, corresponding to 00h00, 01h00 and 02h00 local times in Kenya, from 11 different nights spaced evenly through the period 2011–2012. This enabled the SASKYA project to remain within scope, yet also hopefully provide enough information for routine statistical analyses.

Particular care was taken to choose nights on which the prevailing weather in Kenya was not climatologically anomalous, in order to allow direct comparison between the Africa-LAM output and the climatological statistics for Kenya, as depicted by the ERA-interim reanalyses (as already detailed in Section 2) for the same period. These night-time instances of the model were also chosen to correspond as best as possible to peak astronomical viewing times (i.e. data was chosen for the times of midnight, 01h00 and 02h00 local times). As stated earlier, only forecast data from the 18z model run was used in this work, as it was this model run which performed the "3-D-Var" data assimilation scheme.

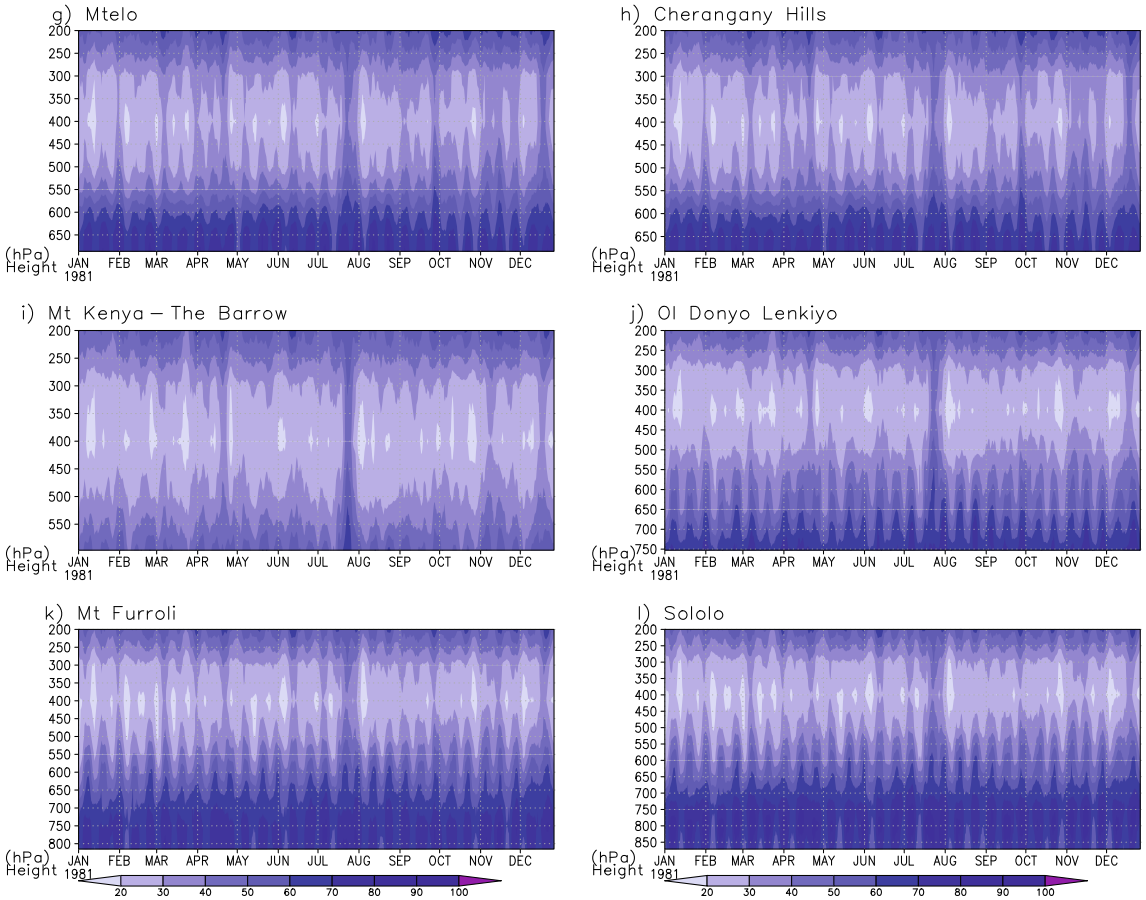

Fig. 10 (continued)

From a quantitative perspective, there were obvious shortcomings in any comparison between the reanalyses and the Africa-LAM because of the small sample size (n) of selected instances of the latter (n=33, but effectively reducing to as low as n=11 due to autocorrelation between successive hourly images at 22, 23 and 00UTC, respectively; Wilks 2005). Hence, days in the middle of each month (approximately 1 month apart) were selected to minimise any effect of persistence or autocorrelation of weather between successive weeks. This disadvantage of a small sample size can be weighed against the merits of having very high-resolution meteorological data for the Kenyan Highlands and also in maintaining the SASKYA project within its initial scope and budget.

Following completion of the above, the UK Met Office "*PP*" files were converted to the World Meteorological Organisation (WMO) netcdf standard file format, using the "XConv-Convsh" software, which was provided for free by the UK Met Office. The open source Grid and Analysis Display *(GrADS)* software was then used to extract, calculate and plot cloud cover and precipitable water vapour (PWV) data for the aforementioned four best-performing candidate sites.

Because of the limited scope (as already mentioned) of this part of the SASKYA project, the results are presented in a separate Appendix 1 at the end of this document. The times and days that were selected for data download are also given in a separate Appendix 2.

4 Consideration of the results and conclusions

A mixture of 30 years (1981–2010) of relatively coarse-grained ERA-interim reanalyses data and 12 months' (2011–2012) of much higher resolution UK Met Office Africa Limited Area Model (Africa-LAM) data were used in an investigation to determine the best possible sites for astronomical observation in Kenya. Cloud cover, precipitable water vapour (specific humidity), vertical velocity, aerosol and wind data were analysed during the investigation.

Both the reanalyses and Africa-LAM data indicate the mountain peaks of Mount Kulal and Ol Donyo Nyiro in the north of Kenya are the most favourable with respect to cloud cover, although a large region bordering and including the Chalbi desert in north-

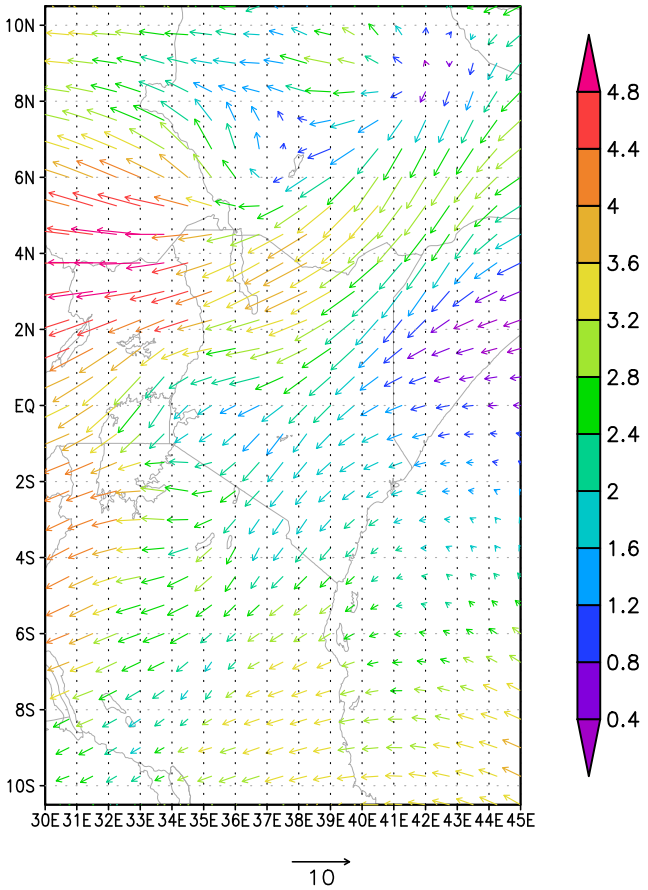

Fig. 11 Average ERA-interim (1981–2010) prevailing wind vectors (direction and velocity, knots) above Kenya at 700 hPa

eastern Kenya (from the mountain peaks of Warges north to Mount Marsabit) is indicated to be reasonably cloud free, with annual mean total cloud cover of around 30 % (equivalent to a photometric night fraction of possibly 50 %). Significant seasonal variation in cloud cover can be expected, however, as well as large inter-annual and inter-decadal oscillations. The prevalence of high cirrus cloud across many parts of Kenya throughout the year may be problematic for any future observatory, however. This may limit the type of optical observations to those that can tolerate some cloud extinction (e.g. differential photometry, imaging and spectroscopy) compared to those that cannot (e.g. near-infrared observations and absolute photometry).

Mean annual PWV values, as determined by both the reanalyses and Africa-LAM are uncomfortably high for all sites (with the exception of The Barrow candidate site on Mount Kenya), with mean values ranging between approximately 10 and 14 mm over the 2000- to 2500-m altitude range. The highest sites are certainly drier (in terms of PWV), but one must ascend to a level of at least 4000 m in order to obtain consistent mean annual PWV values of 5 mm or less. The reanalysis data suggest that the candidate site of "The Barrow" (4192 m) on Mount Kenya is the only place in Kenya where this is achieved for large parts of the year (3.7± 1.1 mm), but construction of a telescopic dome would probably be prohibited here due to its location within a national park. Second on the list, Ol Donyo Nyiro mountain (the next highest site, at 2752 m), performs reasonably well with a mean annual PWV value of 10.7±1.9 mm, but infrastructural issues and a lack of easy access to this mountain may prohibit further investigation as a candidate site.

Analyses of long-term ERA-interim vertical velocities as proxy to determine areas of improved "seeing" conditions (by identifying regions of gently descending air) confirm that the Chabli desert region of northeastern Kenya is again the most favourable region with respect to minimal amounts of turbulence (those associated with diurnal thermal convection currents). A deep turbulent surface boundary layer was identified, however, reaching above 3000 m at most candidate sites. Furthermore, there are important seasonal variations in vertical velocity, so good astronomical seeing conditions cannot be expected anywhere in Kenya all-year round.

Finally, after full consideration of the climatological data, a trade-off between the best possible site in climatological terms, and the practicalities of installing remote equipment in isolated, inaccessible areas with little or no infrastructure will become an important consideration, as well as any local cultural issues pertaining to each mountain region.

Overall, out of a total of 13 original candidate sites across Kenya, the best performing candidate sites, in climatological terms (after the dropping of Mount Kenya off the list) are as follows: Ol Donyo Nyiro, Mount Kulal and Warges. From an infrastructural point of view, however, both Warges and Mount Kulal are considerably more preferable than Ol Donyo Nyiro because

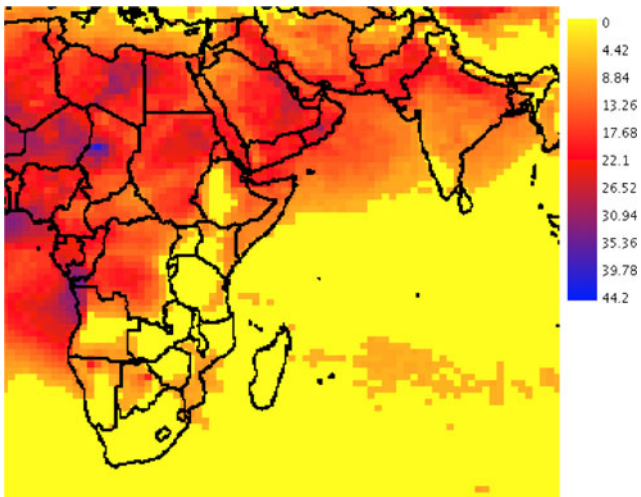

Fig. 12 Maximum aerosol index (×10) from 1981 to 2002 for Eastern Africa and West Indian Ocean, based on TOMS satellite algorithm and as determined using the FriOWL software (Graham 2008a)

of their relative ease of access and nearness to present infrastructure and roads. It was therefore decided in late 2012 that meteorological and astronomical site testing equipment be installed on the summits of (a) Mount Kulal, an undulating ridge, and (b) Warges (a pointed peak). It is also decided that an open eye should be maintained regards Ol Donyo Nyiro mountain or any potential sites in the vicinity of western border of the Chalbi desert.

5 Recommendations for future work

It is recommended that future research of the climatology of mountain sites in Kenya (and in other African countries) utilise the much greater information contained in whole of the Africa-LAM dataset, as well as direct METEOSAT satellite data from EUMETSAT, possibly through the establishment of a dedicated data download, management and dissemination service. As Kenya lies on the equator, not far from the nadir-viewing position of METEOSAT (with up to 1 km image resolution by the SEVIRI sensor), the advantages of obtaining, using and analysing such a resource for astronomical site selection across Africa are considerable. Such a data repository, however, would require resources and investment in order for it to become established and be maintained, but it is recommended that funding opportunities for such be investigated by relevant stakeholders.

The building of a future large telescope in Kenya would also significantly enrich a culture of higher learning in Kenya. It would also benefit students in the neighbouring countries of Uganda, Tanzania, Rwanda and Burundi, who are unlikely to have the same site potential within their borders. SASKYA, therefore, not only increases the opportunity for research in Kenya and train more students in astronomy and physics, enabling students from across Africa to remain on their home continent during the duration of their education and training, but also to make astronomical data available for consumption both in Kenya and across the globe.

Acknowledgments The ECMWF ERA-interim data used in this study/project have been provided by ECMWF and have been obtained from the ECMWF data server. The UK Met Office (UKMO) Limited Area Model for Africa (Africa-LAM) was kindly made available by the UK Met Office, through the British Atmospheric Data Centre (BADC). This research was funded by the Kenya–South Africa Joint Science and Technology Research programme. A grant by the Carnegie Trust for the Universities of Scotland enabled Dr. E. Graham of the University of the Highlands and Islands to travel to South Africa in December 2012 and participate in discussions with the SASKYA team, leading to the decision to install astronomical site testing equipment at *Warges* and *Mount Kulal*. Dr. Graham is grateful for the support of the Carnegie Trust in this regard.

Appendix 1

We were expecting to see broad qualitative visual agreement between the output from the Africa-LAM and the local topography of Kenya. This is confirmed, for example, in Fig. 13, which shows the precipitable water vapour over Kenya, at 00z on 16 August 2011, as determined using the Africa-LAM. The high resolution of this model enables regional climatic features associated with the Rift valley to be discerned [e.g. a north–south-aligned band of higher PWV is apparent, depicted by brighter shades (red and yellow in online version)]. Very low PWV associated with the high peaks of Mount Kenya/Mount Kilimanjaro are also apparent [shown as small concentric regions of darker shades (blue and purple colours in the online version)]. The moister lowland coastal area of eastern Kenya (generally higher PWV values) is also clearly apparent. These topographic features are discernible because PWV varies greatly with height (Morland and Matzler 2007).

Africa-LAM cloud cover

Table 5 presents the average cloud cover statistics for the candidate sites, as determined from the Africa-LAM for the selected days during the period of 2010–2011. These are expressed as an "Africa LAM cloud cover (ALCC) statistic", which is defined here as the average of the model's *bulk cloud fraction (bcc)* variable over all 70 levels of the model, as defined by Eq. 4:

$$\mathrm{ALCC} = \frac{\sum_{1}^{70} \mathrm{bcc}}{70} \tag{4}$$

where *bcc* is the bulk cloud fraction for each of the 70 layers of the Africa-LAM.

The data presented in Table 5 is therefore also a measure of the integrated cloudiness. As detailed earlier in Section 2, however, this vertical integration is *not* the same as total cloud cover because varying amounts of overlapping cloud layers will increase the integrated cloudiness value more greatly than the total cloudiness. Many other varying factors such cloud opacity, thickness, temperature, air pressure, ice/water content and droplet/crystal distribution will also have an unknown influence on the variable. Due to these factors, and also the high number of atmospheric levels in the model, a degree of caution should be applied when considering these as straightforwards percentages of cloud cover. Instead, they may be thought of as average relative values for the selected sites over the analysed nights in question.

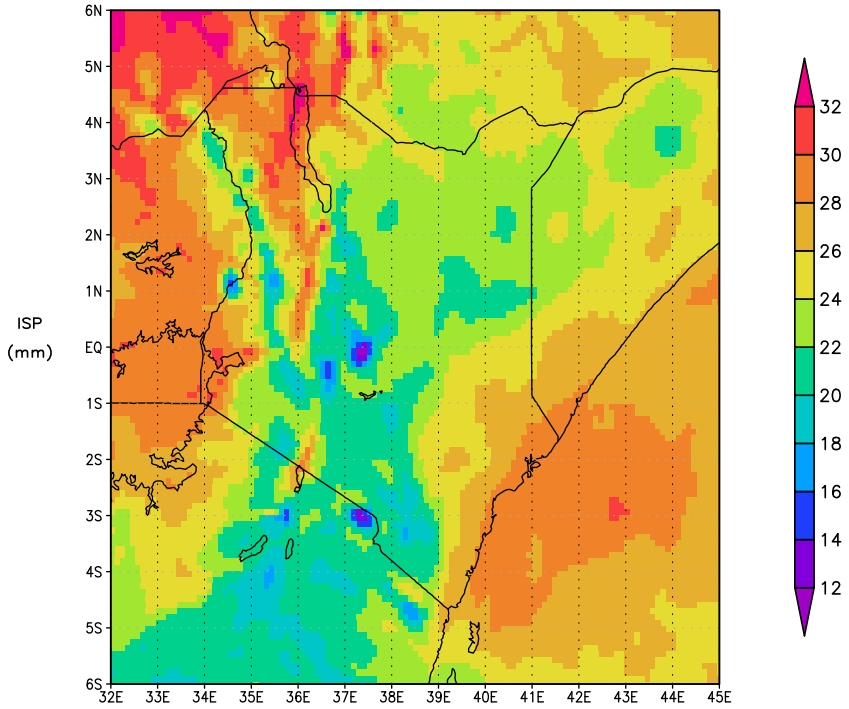

Fig. 13 Precipitable water vapour (specific humidity; kg_{water}/kg_{Air}) map of Kenya, at 00z on 16 August 2011, from the UK Met Office Limited Area Model (*LAM*) for Africa (Met Office, ×200), run at 12 km resolution with 70 vertical levels

Furthermore, because of the limited number of sample nights used in this part of the study, further caution must be applied when considering these results. It is therefore recommended to interpret these data only as rough guides as to the *relative* differences in cloud cover between the four best-performing sites, based on a very limited survey of 11 key nights over the 2010–2011 period.

Keeping these limitations in mind, it can be seen from Table 5 that the values for Mount Kulal, Ol Donyo Nyiro and Warges are all roughly equivalent, ranging from ~32 to 36 %. The very low value of 16.5 % found at Mount Kenya (The Barrow) is because of its great height, as there is less atmosphere to integrate through and the Africa-LAM model may not be able to capture continual thin but local low orographic cloud at this location, despite it being a very high resolution model.

Therefore, it is of our opinion that no firm additional conclusions can be drawn from this analyses, as to whether any of the best-performing SASKYA candidate sites are considerably more or less cloudy than one another, based on the output of the Africa-LAM. On-site measurements using astronomical and meteorological site testing equipment at the candidate sites would be required to refine our knowledge of their characteristics.

A plot of integrated bulk cloud fractions from the Africa-LAM against the ERA-interim values of total cloud cover for each candidate site might be expected to show some level of agreement between the two independently derived variables. However, this task could not be undertaken in the current study, due to the lack of any temporal overlap in the series of each dataset. It is concluded, therefore, that any further deductions on the meso-scale and local meteorology of the candidate sites would therefore need to involve a much larger dataset output from the Africa-LAM or an equivalently resolute model.

Appendix 2: integrated specific humidity

In a similar way to that undertaken when analysing cloud cover output from the Africa-LAM (as described in the preceding section), specific humidity statistics were determined for the same four best-performing SASKYA candidate sites using output from the Africa-LAM. Unfortunately, it was not possible to determine the precipitable water vapour (PWV) for each site using the Africa-LAM model, as the specific heights of each model layer (for the determination of each layer's thickness and thus mass weighting) were not specified in the Africa-LAM humidity files. Thus, a new variable, which was called the integrated specific humidity (ISH), was defined as the vertical summation of the

specific humidity through the 70 levels of the Africa-LAM model, averaged and multiplied by the mean total mass of the atmosphere above the candidate site, as follows:

$$\mathrm{ISH} = \frac{\sum_{z=1}^{z=70} q}{70}\,\overline{M} \tag{5}$$

where q is the specific humidity ($g_{\mathrm{water\ vapour}}/kg_{\mathrm{air}}$), and $\overline{M}$ is the average mass of the atmosphere above each candidate site (calculated by determining the long-term 1981–2010 average atmospheric air pressure at each candidate site using the ERA-interim reanalysis).

Thus, differences between ISH and PWV will occur where the atmospheric layers in the model are of varying thickness and mass. Lacking a suitable alternative in this instance, however, meant that the computation of the ISH was deemed the best option for us, given the circumstances. The resulting ISH values for each site are shown in Table 6 in units of $kg_{\mathrm{water\ vapour}}/m^2$, which is also equivalent to millimetres, the same unit as for PWV.

Looking closely at Table 6, it can be seen that the ISH values are considerably higher than the mean PWV presented for each site in Table 4 (more than double in some instances), based the ERA-interim dataset. This is probably because of the major shortcomings in the method of determining ISH (compared to PWV), as outlined above (as it is unlikely that the ERA-interim model is incorrect in the earlier instance). The largest cause of error is probably due to the incorrect mass weightings per layer of atmosphere. Therefore, it is recommended that the absolute values presented in Table 6 should be ignored in *absolute* terms, but instead be considered in *relative* terms only. In this light, some useful information can still be extracted, namely that standard deviations of ISH amount to only a small fraction of the total ISH signal at each site (unlike what we found for cloud amounts in the previous section), the Mount Kenya site has ISH values of less than half that of most of the other sites (Mount Kulal, Warges), and Ol Donyo Nyiro mountain is somewhat drier than either Mount Kulal or Warges (as also found out in Section 2 using the ERA-interim analysis). These confirm the findings already presented in Table 4 using the ERA-interim reanalysis.

Furthermore, a plot of Africa-LAM ISH values against ERA-interim PWV values (Fig. 14) for all of the original candidate sites shows fairly good agreement (r^2=0.51, significant at 90 % confidence level). This correlation mainly exists, however, because PWV decreases rapidly with height (Morland and Matzler 2007) and our sites cover a range of altitudes. Therefore, a much larger sample size of output statistics (preferably PWV, not ISH) from the Africa-LAM or an equivalently resolute model, compared to ERA-interim data for the same period and presented as anomalies of PWV from their mean, might be a

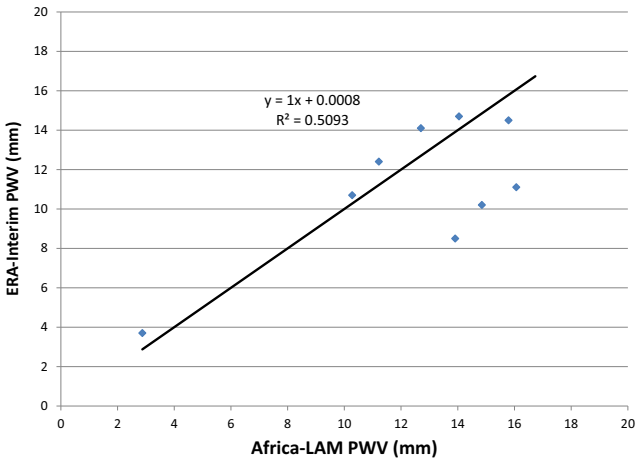

Fig. 14 A plot of Africa-LAM integrated specific humidity (ISH) determined from 33 instances of the model during 2010–11, against long-term (1981–2010) ERA-interim precipitable water vapour (*PWV*) for the four candidate sites of Mount Kulal, Ol Donyo Nyiro, Warges and Mount Kenya (The Barrow)

Table 5 Africa-LAM cloud cover statistics (ALCC)

Name	Altitude (m)	Mean Africa-LAM cloud cover (%)
Mount Kulal	2293	35.8
Ol Donyo Nyiro	2752	34.7
Warges	2688	32.0
Mt. Kenya (The Barrow)	4417	16.5

Table 6 Africa-LAM integrated specific humidity (ISH)

Name	Altitude (m)	Mean ISH (mm)	Median (mm)	10th/90th percentiles	Standard deviation (mm)
Mount Kulal	2293	23.3	23.3	13.3/21.1	5.5
Ol Donyo Nyiro	2752	19.1	20.2	10.6/25.5	4.3
Warges	2688	22.3	22.3	15.9/28.7	5.3
Mt. Kenya (The Barrow)	4417	10.2	10.2	4.3/13.6	3.4

better way of comparing the two such datasets—it is recommended that any future studies attempt this.

Appendix 3

The times and days of the Africa-LAM data that were selected for data download were as follows:

22UTC, 15th June 2011	23UTC, 15th June 2011	00UTC, 16th June 2011
22UTC, 15th July 2011	23UTC, 15th July 2011	00UTC, 16th July 2011
22UTC, 15th August 2011	23UTC, 15th August 2011	00UTC, 16th August 2011
22UTC, 15th September 2011	23UTC, 15th September 2011	00UTC, 16th September 2011
22UTC, 17th October 2011	23UTC, 17th October 2011	00UTC, 18th October 2011
22UTC, 25th December 2011	23UTC, 25th December 2011	00UTC, 26th December 2011
22UTC, 15th January 2012	23UTC, 15th January 2012	00UTC, 16th January 2012
22UTC, 14th February 2012	23UTC, 14th February 2012	00UTC, 15th February 2012
22UTC, 15th March 2012	23UTC, 15th March 2012	00UTC, 16th March 2012
22UTC, 15th April 2012	23UTC, 15th April 2012	00UTC, 16th April 2012

References

Agabi A, Aristidi E, Azouit M, Fossat E, Martin F, Sadibekova T, Vernin J, Ziad A (2006) First whole atmosphere night-time seeing measurements at Dome C, Antarctica. Publ Astron Soc Pac 118(840):344–348

Anyah RO, Semazzi FH (2007) Variability of East African rainfall based on multiyear RegCM3 simulations. Int J Climatol 27(3):357–371

Casals P, Beniston M (2001) Climatological analysis of seeing conditions at the site of the European Southern Observatory (ESO) in Paranal, Chile. Report by the Department of Geosciences, University of Fribourg, Switzerland. Contract no. 61243/ODG/00/8543/GWI/LET

Chevallier F, Kelly G, Simmons AJ, Uppala S, Hernandez A (2003) High clouds over oceans in the ECMWF 15-year and 45-year re-analyses. ERA-40 Project Report Series No.11. ECMWF, Shinfield Park, Reading, England. Available at: http://www.ecmwf.int/publications/library/do/references/list/192. Accessed May2008

Dee DP, Uppala SM, Simmons AJ, Berrisford P, Poli P, Kobayashi S, Vitart F (2011) The ERA-interim reanalysis: configuration and performance of the data assimilation system. Q J R Meteorol Soc 137(656):553–597

Ehgamberdiev SA, Baijumanov AK, Ilyasov SP, Sarazin M, Tillayev YA, Tokovinin AA, Ziad A (2000) The astroclimate of Maidanak Observatory in Uzbekistan. Astron. Astrophys. Suppl. Ser. 145, 293–304

Environment Canada (2014) Seeing forecast for astronomical purposes [online]. Available at: http://weather.gc.ca/astro/seeing_e.html. Accessed: 25 Jan 2015

European Southern Observatory ESO (2007) OWL Concept design report: phase A design review (OWL-TRE-ESO-0000-0001 Issue 2: Chapter 14: site characterisation), Garching, Germany

European Southern Observatory ESO (2015) *Astroclimatology* [online], Available at: <http://www.eso.org/gen-fac/pubs/astclim/>. Accessed 22 Jan 2015

Giordano P, Sarazin M (1994) Survey of airborne particle density and the ageing of mirror coatings in the open air at the VLT Observatory. Proc Int Soc Opt Eng (SPIE) 2199:977–985, SPIE 2199–977

Graham E, Sarazin M, Beniston M, Collet C, Hayoz M, Neun M, Casals P (2005) Climate-based site selection for a Very Large Telescope using GIS techniques. Meteorological Applications 12(01), 77-81

Graham E (2008a) The FriOWL Guide: A site selection tool for extremely large telescopes using climate data. Forschungsbericht Nr. 2008-09-MW, Institut fur Angewandte Physik, Universitat Bern, 256pp.

Graham (2008b) Applications of FriOWL: the Paranal and La Silla astroclimate report. IAP Research Report, No. 2008-08-MW, Institut für angewandte Physik, Universität Bern, 85pp

Graham E, Sarazin M, Matzler C (2011) Using re-analysis model data ("FriOWL") to analyse climate trends related to astroclimatology of Paranal and La Silla. Rev Mex Astron Astrofis (Ser Conf) 41:12–15

Hastenrath S (1995) Glacier recession on Mount Kenya in the context of the global tropics. Bull Inst Fr Etudes Andines 24:633–638

Hastenrath S, Kruss PD (1992) The dramatic retreat of Mount Kenya's glaciers between 1963 and 1987: greenhouse forcing. Ann Glaciol 16:127–133

Herman JR, Bhartia PK, Torres O, Hsu C, Seftor C, Celarier E (1997) Global distribution of UV-absorbing aerosols from Nimbus 7/TOMS data. J Geophys Res 102(D14):16911–16922

Janowiak JE (1988) An Investigation of Interannual Rainfall Variability in Africa. Journal of Climate 1(3):240-255

Kalnay E, Kanamitsu M, Kistler R, Collins W, Deaven D, Gandin L, Iredell M, Saha S, White G, Woollen J, Zhu Y, Chelliah M, Ebisuzaki W, Higgins W, Janowiak J, Mo KC, Ropelewski C, Wang J, Leetmaa A, Reynolds R, Jenne R, Joseph D (1996) The NCEP/NCAR Reanalysis Project. Bull Am Meteorol Soc 77:437–471

Kaser G, Hardy DR, Mölg T, Bradley RS, Hyera TM (2004) Modern glacier retreat on Kilimanjaro as evidence of climate change: observations and facts. Int J Climatol 24(3):329–339

Koffi E, Graham E, Mätzler A (2013) The water vapour flux above Switzerland and its role in the August 2005 extreme precipitation and flooding. Meteorol Z 22(3):328–341

Lawrence JS, Ashley MCB, Tokovinin A, Travouillon T (2004) Exceptional astronomical seeing conditions above Dome C in Antarctica. Nature 431:278–281. doi:10.1038/nature02929

Lumb FE (1970) Topographic influences on thunderstorm activity near Lake Victoria. Weather 25(9):404–410

Marchant R, Mumbi C, Behera S, Yamagata T (2007) The Indian Ocean dipole—the unsung driver of climatic variability in East Africa. Afr J Ecol 45(1):4–16

Masciadri E, Egner SE (2004) First complete seasonal variation study of the 3D optical turbulence above San Pedro Mártir Observatory. Proc Int Soc Opt Eng (SPIE) 5490:818–829

Mastny L (2000) Melting of earth's ice cover reaches new high. Worldwatch Institute News Brief (6), 5pp

Maxwell D, Fitzpatrick M (2012) The 2011 Somalia famine: context, causes, and complications. Global Food Secur 1(1):5–12

Morland JC, Matzler C (2007) Spatial interpolation of GPS Precipitable water vapour measurements made in the Swiss Alps. Meteorol Appl 14:15–26

Nicholson SE (1996) A review of climate dynamics and climate variability in Eastern Africa. The limnology, climatology and

paleoclimatology of the East African lakes. Gordon and Breach, Amsterdam, pp 25–56

Sarazin M (1997) Characterisation of the optical properties of atmospheric turbulence: methods for the evaluation of an astronomical site. European Southern Observatory, internal document, 21 November 1997, Garching, Germany (revision of a partial translation from an original French PhD thesis, 1992) (online). http://www.eso.org/gen-fac/pubs/astclim/papers/ms-pubs/. Accessed 4 December 2013

Siher EA, Ortolani S, Sarazin MS, Benkhaldoun Z (2004) Correlation between TOMS aerosol index and the astronomical extinction. Proc Int Soc Opt Eng (SPIE) 5489-13, 138–145

Tapia M (1992) Ten years of weather and observing statistics in San Pedro Mártir, Baja California, Mexico. Rev Mex Astron Astrofis 24: 179–186

Torres O, Bhartia PK, Herman JR, Sinyuk A, Ginoux P, Holben B (2002) A long term record of aerosol optical thickness from TOMS observations and comparison to AERONET measurements. J Atmos Sci 59:398–413

Trenberth KE (1984) Signal versus noise in the Southern Oscillation. Mon Weather Rev 112(2):326–332

UK Meteorological Office UKMO (2012) Limited Area Model for Africa (Africa-LAM), NCAS British Atmospheric Data Centre (online). http://badc.nerc.ac.uk/view/badc.nerc.ac.uk__ATOM__DE_2f0971ba-f76d-11df-8151-00e081470265. Accessed 29 October 2014

Uppala SM, Kållberg PW, Simmons AJ, Andrae U, da Costa Bechtold V, Fiorino M, Gibson JK, Haseler J, Hernandez A, Kelly GA, Li X, Onogi K, Saarinen S, Sokka N, Allan RP, Andersson E, Arpe K, Balmaseda MA, Beljaars ACM, van de Berg L, Bidlot J, Bormann N, Caires S, Chevallier F, Dethof A, Dragosavac M, Fisher M, Fuentes M, Hagemann S, Hólm E, Hoskins BJ, Isaksen L, Janssen PAEM, Jenne R, McNally AP, Mahfouf J-F, Morcrette J-J, Rayner NA, Saunders RW, Simon P, Sterl A, Trenberth KE, Untch A, Vasiljevic D, Viterbo P, Woollen J (2005) The ERA-40 re-analysis. Q J R Meteorol Soc 131:2961–3012. doi:10.1256/qj.04.176

Wilks D (2005) Statistical methods in the atmospheric sciences, 2nd edn. International Geophysics. Academic Press, 648pp

Yin X, Nicholson S, Ba MB (2000) On the diurnal cycle of cloudiness over Lake Victoria and its influence on evaporation from the lake. Hydrol Sci J 45(3):407–424. doi:10.1080/02626660009492338

Ziad A (2012) Astronomical observations through atmospheric turbulence. Adaptive Optics and the Atmosphere Summer School, Sutherland, South Africa